RESEARCH ARTICLE

Mutations in Tomato 1-Aminocyclopropane Carboxylic Acid Synthase2 Uncover Its Role in Development beside System II Responses

Kapil Sharma, Soni Gupta[1], Supriya Sarma, Meenakshi Rai, Yellamaraju Sreelakshmi*, Rameshwar Sharma*

Repository of Tomato Genomics Resources, Department of Plant Sciences, University of Hyderabad, Hyderabad-500046, India

[1]Current address: Genetics and Plant Breeding, CSIR-Central Institute of Medicinal and Aromatic Plants, Lucknow-226015, India

Corresponding authors: rameshwar.sharma@gmail.com; syellamaraju@gmail.com

Short title: Tomato ACS2 regulates broad developmental responses

One sentence summary: Genetic and functional analysis of *ACS2* mutants reveal high/low ethylene emission oppositely modulates developmental processes and metabolite profiles in tomato.

The authors responsible for the distribution of materials integral to the findings in this article in accordance with the policy described in the instructions for authors (www.plantcell.org) are Rameshwar Sharma (rameshwar.sharma@gmail.com) and Yellamaraju Sreelakshmi (syellamaraju@gmail.com).

ABSTRACT

The role of ethylene in plant development is mostly inferred from its exogenous application. The usage of the mutants affecting ethylene biosynthesis proffers a better alternative to decipher its role. In tomato, 1-aminocyclopropane carboxylic acid synthase2 (ACS2) is a key enzyme regulating ripening-specific ethylene biosynthesis. We characterized two contrasting *acs2* mutants; *acs2-1* overproduces ethylene, has higher ACS activity, and increased protein levels, while *acs2-2* is an ethylene under-producer, displays lower ACS activity, and protein levels than wild type. Consistent with high/low ethylene emission, the mutants show opposite phenotypes, physiological responses, and metabolomic profiles than the wild type. The *acs2-1* showed early seed germination, faster leaf senescence, and accelerated fruit ripening. Conversely, *acs2-2* had delayed seed germination, slower leaf senescence, and prolonged fruit ripening. The phytohormone profiles of mutants were mostly opposite in the leaves and fruits. The faster/slower senescence of *acs2-1*/*acs2-2* leaves correlated with the endogenous ethylene/zeatin ratio. The genetic analysis showed that the metabolite profiles of respective mutants co-segregated with the homozygous mutant progeny. Our results uncover that besides ripening, ACS2 participates in vegetative and reproductive development of tomato. The distinct influence of ethylene on phytohormone profiles indicates intertwining of ethylene action with other phytohormones in regulating plant development.

INTRODUCTION

Ethylene is a simple gaseous molecule that also acts as a natural plant hormone. It participates in a multitude of development processes such as seed germination, organ senescence, biotic and abiotic stresses, and fruit ripening (Abeles et al., 1992). The ethylene-mediated stimulation of the ripening process is restricted to the climacteric fruits, where a surge in respiration marks the onset of ripening. The respiratory surge is preceded by increased ethylene biosynthesis that triggers the ripening (Grierson, 2013). Antagonistically, mutations, or the chemical treatments that block ethylene biosynthesis/perception, abolish or delay the ripening of climacteric fruits (Brady, 1987; Martínez-Romero et al., 2007). For studies on climacteric fruit ripening, tomato (*Solanum lycopersicum*) has emerged as a preferred model system due to the availability of several monogenic mutants affecting the ripening process and ease of transgenic manipulations (Barry, 2014; Seymour et al., 2013).

The studies carried out on tomato mutants defective in fruit ripening have established a hierarchical genetic regulation of the ripening process. One of the extensively investigated mutant is *ripening-inhibitor* (*rin*) that lacks almost all ripening associated processes like the accumulation of lycopene, softening of fruits, and a climacteric burst of ethylene (Tigchelaar et al., 1978). The *RIN* gene encodes a MADs-type transcriptional factor, which positively regulates the onset of the ripening process (Vrebalov et al., 2002). RIN is known to function as a protein dimer consisting of two monomeric subunits. RIN directly binds to the promoters of a large number of ripening-related genes, including those involved in ethylene biosynthesis (Fujisawa et al., 2012; Qin et al., 2012). Consequently, the *rin* mutant fails to induce the genes associated with the ripening process. The *rin* mutant does not ripen on exposure to the exogenous ethylene, though it retains some ethylene-induced responses that are independent of RIN (Lincoln and Fischer, 1988).

In addition to *RIN*, other genes such as *COLORLESS NONRIPENING* (*CNR*) and *NONRIPENING* (*NOR*) identified by respective mutant analysis regulate tomato ripening, including ethylene biosynthesis and have a complex interaction with RIN. CNR is an essential factor for DNA binding of RIN and, at the same time, is the target of RIN (Martel et al., 2011). NOR seems to have a dual action in the regulation of ripening as it acts both upstream and downstream of RIN (Osorio et al., 2011). The reduced expression of ethylene biosynthesis gene *ACS2* in *Cnr* and *Nor* mutants is associated with hyper-H3K27me3 marks in *ACS2* gene loci (Gao et al., 2019). Other ripening regulatory genes such as *TOMATO AGAMOUS-LIKE* (*TAGL*)

(Vrebalov et al., 2009; Itkin et al., 2009), *HD-ZIP homeobox protein* (*LeHB1*) (Lin et al., 2008), *APETALA2* (*SlAP2a*; Karlova et al., 2011) are also necessary for ethylene induction and ripening in tomato.

The paramount role of ethylene in regulating tomato ripening is also highlighted by the loss of ripening in tomato *Nr* mutant. The *Nr* mutant encodes a truncated ethylene receptor ETR3, consequently compromised in ethylene perception (Wilkinson et al., 1995). The ripening can be restored in transgenic *Nr* fruits by antisense inhibition of mutated gene suggesting receptor inhibition model of ethylene action (Hackett et al., 2000). Likewise, overexpression of *EIL1* (*EIN3*-like transcription factor) restores ripening in the *Nr* (Chen et al., 2004), indicating the operation of normal ethylene signal transduction in the mutant. Though the transcript levels of *ETR3* and *ETR4* increases during tomato ripening (Liu et al., 2015), the ETR3 and ETR4 receptors are dephosphorylated due to elevated ethylene levels, thus allowing ethylene signal transmission during ripening (Kamiyoshihara et al., 2012). The mutations in tomato *ETR1*, *ETR4*, and *ETR5* genes had a differential effect on the fruit ripening, probably by affecting their ethylene sensitivity (Okabe et al., 2011; Mubarok et al., 2019). The regulated expression of Arabidopsis *ethylene resistant1-1* (*etr1-1*) mutant gene conferred ethylene insensitivity in tomato fruits, similar to its parental line in Arabidopsis, blocking normal ripening of fruits (Gallie, 2010).

The elegant studies initially conducted on wounded apple fruit tissues uncovered the ethylene biosynthesis pathway in higher plants named as Yang cycle (Adams and Yang, 1979). The ethylene is derived from C-3,4 of amino acid methionine, which is first converted to S-adenosylmethionine (SAM) by SAM synthase. SAM, a common precursor of many biosynthetic pathways, is converted to 1-aminocyclopropane carboxylic acid (ACC) by ACC synthase (ACS). The conversion of ACC to ethylene is catalyzed by ACC oxidase (ACO) in the presence of oxygen. The 5-methylthioribose released during ACC formation is recycled to methionine to prevent depletion of methionine pool. ACC can also be conjugated with malonic acid to form malonyl-ACC (MACC) by ACC malonyltransferase (Hoffman et al., 1982). The formation of ACC by ACS constitutes the first committed step in ethylene biosynthesis.

ACS is considered as the rate-limiting enzyme in the ethylene biosynthesis pathway. In tomato, ACS is encoded by a multigene family consisting of at least nine genes (*ACS1A, ACS1B, and ACS2-8*) and five putative genes (Liu et al., 2015). ACS proteins are classified as three types based on the presence or absence of phosphorylation sites in their C-terminal sequence. Type 1

ACS isoforms have an extended C-terminal region containing CDPK and MAPK phosphorylation sites (SlACS1A, SlACS1B, SlACS2, SlACS6), whereas type 2 ACS have only a CDPK phosphorylation site (SlACS3, SlACS7, SlACS8), and type 3 altogether lack a phosphorylation site (SlACS4, SlACS5) (Lin et al., 2009). Biochemical studies on Arabidopsis ACS isoforms revealed that though ACS can form homodimers and heterodimers, except ACS7, only heterodimers formed between the same types are functional (Tsuchisaka and Theologis, 2004). However, ACS heterodimerization and the post-transcriptional phosphorylation enhance the diversity of action of ACS during plant growth and development (Tsuchisaka et al., 2009).

During tomato fruit development and ripening, *ACS* genes are differentially regulated by endogenous mechanisms and ethylene mediated autocatalytic induction. During tomato fruit development, the expressions of *ACS* genes considerably differ in system-I and system-II responses (Klee and Giovannoni, 2011). During system-I that is confined to the fruit expansion phase, *ACS* genes are moderately expressed. During system-II, which marks the ripening induction, *ACS2, ACS4,* and *ACS6* are highly expressed (Nakatsuka et al., 1998; Barry et al., 1996, 2000; Van de Poel et al., 2012). The strong association between ripening and increased *ACS2* expression was indicated by the total suppression of tomato fruit ripening by antisense inhibition of the *ACS2* gene (Oeller et al., 1991). The high expression of *ACS2* during ripening likely results from the binding of transcription factors like RIN (Ito et al., 2008) and TAGL1 (Itkin et al., 2009) to the promoter of the *ACS2* gene. Genome-wide analysis of DNA methylation demonstrated that tomato ripening is associated with the demethylation of several genes promoters, including *ACS2* and the receptors *ETR3* and *ETR4* (Zhong et al., 2013). Based on the absence of binding of TAGL to *ACS4* promoter, Itkin et al. (2009) suggested *ACS2* is the primary ethylene biosynthesis gene, regulating tomato ripening. The kinetic analysis of ethylene biosynthesis, ACC accumulation, ACS activity, and *ACS* genes expression indicated that during tomato ripening ACS4 and ACS6 are less important, whereas ACS2 seems to be the main biosynthetic enzyme as its expression is ethylene dependent and mainly occurs during system 2 (Barry et al., 2000; Van der Poel et al., 2014).

While the *ACS2* gene, along with other ethylene biosynthesis genes, seemingly contributes to the climacteric rise of ethylene during tomato ripening, the information about its role in other developmental processes of tomato is limited. The paucity of information about its role stems from the near absence of tomato mutants compromised in the ethylene biosynthesis pathway. Here we

describe isolation and characterization of two novel *ACS2* mutants of tomato having diametrically opposite effects on ethylene emission. The *acs2-1* mutant has high ethylene emission, and *acs2-2* shows reduced ethylene emission. We show that stimulation/reduction of ethylene emission affects several developmental processes right from seed germination to fruit ripening. We also show that variation in ethylene emission affects hormonal and metabolome profiles in an opposite manner.

RESULTS

Identification and confirmation of mutations in *ACS2* gene

To identify *ACS2* gene mutants, we screened genomic DNA from 9,144 ethyl methane sulfonate-mutagenized M_2 tomato plants by TILLING. The screening was restricted to the fourth exon of the *ACS2* gene, which was predicted by CODDLE to be prone to deleterious mutations **(Supplemental Figure 1)**. In total, nine *ACS2* mutant alleles were identified **(Supplemental Table 1)**, of which two alleles named *acs2-1* (plant line M82-M3-112**)** and *acs2-2* (plant line M82-M2-162A) **(Supplemental Table 2)** were characterized in detail. The sequencing of the full-length gene, including promoter, revealed two exonic and three intronic mutations in *acs2-1*, and one intronic and two promoter-localized mutations in *acs2-2* **(Figure 1A, Supplemental Table 2)**. The homozygous mutant lines were characterized in M_6 generation and backcrossed twice to parent M82 plants. The genetic segregation analysis showed that *acs2-1* and *acs2-2* were inherited as a monogenic Mendelian trait. The segregation of mutation in F_2 progeny was monitored by CEL-I endonuclease assay (Mohan et al., 2016) [*acs2-1* BC_1F_2- total plants 120, 29 (*acs2-1*/*acs2-1*), 61 (*ACS2*/*acs2-1*), and 30 (*ACS2*/*ACS2*), ratio 1:2:1, χ^2 (0.224) P = 0.62]; [*acs2-2* BC_1F_2- total plants 108, 25 (*acs2-2*/*acs2-2*), 56 (*ACS2*/*acs2-2*), and 27 (*ACS2*/*ACS2*), ratio 1:2:1, χ^2 (0.101) P = 0.95] **(Supplemental Table 3)**. For the majority of fruit ripening experiments, we compared respective mutants with parental wild type (WT), and BC_1 backcrossed progeny.

In silico analysis predicted gain-of-function/loss-of-function for *acs2* mutants

The splice site analysis by NetGene2 server (http://www.cbs.dtu.dk/services/NetGene2/) predicted that A398G (K100=) mutation located in *acs2-1* at 5′ splice site terminating the second exon leads to more efficient splicing of mRNA (WT - 0.74; *acs2-1* - 1.00) that in turn may enhance its transcript level **(Supplemental Figure 2)**. The T2119A mutation leading to valine (neutral non-polar amino acid) to glutamic acid (acidic polar amino acid) (V352E) change is localized in α-helix of ACS2 (Tarun et al., 1998). The computational protein modeling and 3D protein stability analysis indicated that V352E change affects the bonding and folding pattern, improving the stability of ACS2-1 protein (**Figure 1B**, **Supplemental Table 4, 5).** Taken together, enhanced transcript level and stable ACS2-1 protein may lead to a gain-of-function hypermorphic mutation.

It is reported that $C(A/T)_8G$ sites also have an affinity for RIN binding (Fujisawa et al., 2013). In the *acs2-2* mutant, T-106A mutation is located in $C(A/T)_9G$ location, therefore it is

unlikely that it may have disrupted RIN binding site. However, the T-106A mutation disrupts a SOC1 binding site, and gains an AZF binding site, a Zinc finger, C2H2-type transcription factor negatively regulating ABA-mediated responses (Kodaira et al., 2011; tomato homolog Solyc04g077980.1) (**Supplemental Table 6, Supplemental dataset 1**). The T-382A mutation is located at a methylated CpG site that shows a reduction in methylation during ripening (**Supplemental Table 7, Supplemental dataset 2**) (http://ted.bti.cornell.edu/cgi-bin/epigenome/home.cgi). It is plausible that the above mutations in the promoter region reduce the affinity of regulatory transcription factors, thus compromising the *acs2-2* gene expression, and thus resulting in a loss-of-function phenotype. Phenotype characterization of mutants affirmed the notion that *acs2-1* is a gain-of-function, and *acs2-2* is a loss-of-function mutation.

***acs2-1* shows faster seed germination than WT**

In *acs2-1*, the onset of seed germination was 12 h earlier than WT, whereas it was delayed by 12 h in *acs2-2*. The time course and attainment of full germination also followed the above pattern, with *acs2-1* attaining 50% germination at 35 h, WT at 55 h, and *acs2-2* at 77 h **(Figure 1C)**. The ethylene emission from respective mutant seedlings also showed a similar pattern. Three-day old seedlings showed higher emission (280%) from *acs2-1* and lower emission (40%) from *acs2-2* than WT **(Figure 1D)**. The mutant seedlings showed a similar difference in the growth inhibition response with *acs2-1* being more sensitive and *acs2-2* less sensitive than WT to a similar dosage of external ethylene **(Figure 1E and 1F)**.

***acs2-1* and *acs2-2* mutants show distinct effects on plant morphology**

During vegetative growth, *acs2-1* plants displayed faster growth, elongated internodes, and higher ethylene emission from detached leaves than WT (**Figure 2A and 2C**). In contrast, *acs2-2* plants exhibited slightly slower growth and lower ethylene emission from leaves than WT (**Figure 2B and 2C**).**)**. Consistent with ethylene emission, the detached mutant leaves showed faster (*acs2-1*) and slower (*acs2-2*) loss of coloration than WT **(Figure 2D)**. The level of chlorophylls and carotenoids similarly differed from WT **(Supplemental Figure 3)**. The hormonal profiling of *acs2-1* leaves showed up-regulation of jasmonic acid (JA), ABA, methyl jasmonate (MeJA), and down-regulation of IAA, IBA, salicylic acid (SA), and zeatin than WT. In contrast, the hormonal profile of *acs2-2* was closer to WT barring lower level of SA and a higher level of zeatin **(Figure 2E and 2F)**. Principal component analysis of 69 primary metabolites identified **(Supplemental dataset 3)** in mutant leaves showed a distinct difference in metabolite levels than WT **(Figure**

2G). The levels of the majority of metabolites were altered in *acs2-1* and *acs2-2* compared to WT. In general, more metabolites were downregulated in *acs2-1* than *acs2-2* **(Figure 2H)**. The key metabolites of the TCA cycle, such as citrate, isocitrate, and malate, showed opposite levels indicating a differential effect of *acs2-1* and *acs2-2* on the TCA cycle. While levels of several amino acids were high in *acs2-2*, barring threonine, other amino acids showed lower abundance in *acs2-1* than WT.

***acs2-1* shows accelerated ripening and onset of fruit senescence**

Both *acs2* mutant also affected the development of reproductive organs. The *acs2-1* plants had more flowers with a higher fruit set (8±1) per truss than WT (5±1). In contrast, the *acs2-2* plants had fewer flowers and a lower fruit set (4±1) per truss than WT (5±1) (**Figure 3A**, **Supplemental Table 8**). The sepals of *acs2-1* fruits were long, straight, and less green, while WT fruit had curly and green sepals. These results indicate that *acs2-1* mutation accelerates the overall development of plants and enhances fruit yield, and *acs2-2* has the opposite phenotype.

The fruits of *acs2-1* showed accelerated development reaching the mature green (MG) stage by 31 days from anthesis (dpa) **(Figure 3B and 3C)**. Post-MG stage, the *acs2-1* showed accelerated transition through different ripening stages attaining red ripe (RR) stage by 38 dpa. The on-vine RR stage of *acs2-1* fruits was severely short (8 days) with onset of on-vine fruit senescence (FS) at 46 dpa. Though WT and *acs2-2* fruits reached the MG stage nearly at the same time (WT- 39 dpa; *acs2-2*- 40 dpa), the transition of *acs2-2* fruits through different ripening stages was much longer than the WT **(Figure 3C and 3D)**. Post-RR stage, the onset of FS was significantly delayed in *acs2-2* (40 days) than WT (25 days) The *acs2-1* fruits also emitted more ethylene at turning (TUR) (185%) stage than WT. In contrast, *acs2-2* fruits had lower ethylene emission at TUR (76%) and RR (57%) stages than WT **(Figure 3E)**. The respiratory CO_2 emission from the *acs2-1*, *acs2-2*, and WT fruits followed a pattern similar to ethylene, indicating a linkage between these two processes **(Figure 3F)**.

The fruits of *acs2-1* were less firm than WT at TUR and RR stages, while fruits of *acs2-2* were more firm than WT **(Supplemental Figure 4)**. The ripened fruits of *acs2-1* were smaller, and those of *acs2-2* were bigger in size than WT (**Figure 3B).** The analysis of homozygous backcrossed progeny of *acs2-1* and *acs2-2* plants showed a near similar ethylene emission and ripening patterns as described above for the mutants (**Figure 3 C, 3D, and 3E)**. The *acs2* mutation also had a minor effect on the °Brix and pH value of the fruits **(Supplemental Figure 4)**.

Mutation in *acs2-1* leads to increased ACC levels, ACS, and ACO activities

In plants, ethylene synthesis is a two-step process, wherein S-adenosyl L-methionine is converted to 1-aminocyclopropane carboxylic acid (ACC) by ACC synthase (ACS). In the next step, ACC oxidase (ACO) converts ACC to the final end-product ethylene (Yang and Hoffman, 1984). We determined whether higher/lower ethylene emission from *acs2* mutant fruits also correlated with *in vivo* levels of ACC. Consistent with higher ethylene emission, at all ripening stages, in *acs2-1,* the ACC level was higher, whereas in *acs2-2* ACC level was lower than WT **(Figure 4A)**. *In vivo,* ACC is also conjugated to malonic acid to form malonyl-ACC (MACC) by ACC malonyltransferase (Hoffman et al., 1982). Similar to higher ACC levels, the level of MACC was also higher in *acs2-1,* whereas *acs2-2* had a lower level of MACC compared to WT **(Figure 4B)**. To ascertain whether higher/lower ACC levels in mutants reflected the ACC synthase enzyme activity, the ACS activity of mutants and WT fruits was *in vitro* assayed. In conformity with ethylene emission pattern, the ACS activity was 2-fold higher in the *acs2-1,* and it was half in *acs2-2* compared to WT **(Figure 4C)**. We next examined whether higher/lower ACC levels also influenced the activity of the next enzyme- ACO. Even the ACO activity was significantly higher in *acs2-1,* whereas *acs2-2* had lower ACO activity **(Figure 4D)**.

***acs2-1* mutant shows 5-fold high ACS2 protein level than WT**

To determine whether *acs2* mutations influenced ACS2 protein levels, we raised polyclonal antibodies against ACS2 using a synthetic peptide specific to ACS2 protein, and the antibody specificity was confirmed against the peptide **(Supplemental Figure 5)**. In ripening tomato pericarp, the level of ACS protein is estimated to be <0.0001% of the total soluble protein (Bleecker et al., 1986). Consistent with its low abundance, we could not detect ACS2 protein on the Western blot on the direct loading of supernatants from the fruit homogenates**.** Therefore, we purified the IgG fraction from antiserum and immunoprecipitated ACS2 protein to enrich it before Western blot analysis **(Supplemental Figure 6).** The decline in ACS activity in the supernatant after immunoprecipitation indicated the specificity of antibodies toward ACS2 protein. The Western blot analysis revealed no discernible ACS2 protein band in MG and TUR fruits of *acs2-1, acs2-2,* and WT. Only in RR fruits, a single band of 55 kD was detected corresponding to the reported molecular size of tomato ACS2 protein in *acs2-1* and WT (Rottmann et al., 1991). A more prominent band in *acs2-1* compared to WT indicated that it is enriched in ACS2 protein. In contrast, a very faint band in *acs2-2* RR fruits indicated a highly reduced ACS2 protein level

(Supplemental Figure 6). To ascertain the relative amount of ACS2 protein in acs2-*1*, *acs2-2*, and WT RR fruits, we subjected the samples to serial dilution. Matching the intensity of bands of serially diluted proteins indicated that the level of ACS2 protein in WT was about 4-fold less than *acs2-1*. A similar dilution comparison revealed that the ACS2 protein level in *acs2-2* was about 4-fold lower than the WT. These results indicated that similar to differences in ethylene emission, the levels of ACS2 protein in *acs2-1*, WT, and *acs2-2* were in the proportion of 4:1:0.25, respectively **(Figure 4E and 4F)**. The differences in the ACS2 protein levels also support that *acs2-1* is a gain-of-function mutant, while *acs2-2* is a loss-of-function mutation.

It is believed that ACS2 protein stability is regulated by protein phosphorylation at a conserved Ser-460 residue (Tatsuki and Mori, 2001; Kamiyoshihara et al., 2010). Therefore, we examined whether the mutation affected the phosphorylation status of ACS2 protein using the phospho-ser antibody. Considering that ACS2 protein level widely varies in *acs2-1*, WT and *acs2-2*, the gel was run with 20 µg WT protein, 5 µg *acs2-1* protein, and 80 µg *acs2-2* protein, to have an equal amount of ACS2 protein in each lane. At equal levels of ACS2 protein loading, the *acs2-1*, *acs2-2*, and WT lanes showed an equal amount of phosphorylated ACS2 protein, indicating that mutations did not affect the ACS2 phosphorylation **(Figure 4G)**.

***acs2* mutations alter phytohormones level in fruits**

While ethylene is the major hormone regulating fruit ripening in tomato, little is known about its interaction with other hormones. The analysis of *acs2* mutant fruits revealed that ethylene significantly influenced the level of other plant hormones. The levels of zeatin, ABA, JA (Barring MG), MeJA, and SA were higher in *acs2-1* fruits than WT at all stages of ripening. Contrastingly, the IAA level was lower at MG, but at the TUR and RR stage, both WT and *acs2-1* had a nearly similar level (**Figure 5A**). Importantly, analysis of homozygous *acs2-1*/*acs2-1* F_2 plants revealed similar upregulation of zeatin, ABA, JA, MeJA, and SA at all stages of ripening compared to F_2 WT (*ACS2/ACS2*). The JA level in heterozygous (*ACS2*/*acs2-1*) at MG and TUR, and WT (*ACS2/ACS2*) F_2 plants at TUR, were below the limit of detection. Contrasting to *acs2-1*, and compared to WT, the levels of ABA, and SA were lower in *acs2-2* (Barring MG), as well as in homozygous (*acs2-2*/*acs2-2*) F_2 plants at all stages of ripening. The levels of MeJA, JA (at RR), and zeatin (at MG, TUR) was also lower than WT in homozygous (*acs2-2*/*acs2-2*) F_2 plants. The IAA level in homozygous (*acs2-2*/*acs2-2*) F_2 plants (In *acs2-2* only at TUR) and was higher than

the WT at all stages of ripening. **(Figure 5A)**. These results indicate an opposite influence of *acs2-1* and *acs2-2* on the level of other hormones during tomato ripening.

***acs2-1* mutation enhances carotenoids accumulation in fruits**

The onset, progression, and completion of tomato ripening are visually monitored by the change of color imparted by carotenoids. A total of 11 carotenoids; phytoene, phytofluene, ζ-carotene, lycopene, δ-carotene, α-carotene, lutein, γ-carotene, β-carotene, zeaxanthin, and neoxanthin were detected. However, only phytoene, lycopene, lutein, and β-carotene were detected at all stages of ripening. In homozygous (*acs2-1*/*acs2-1*) F_2 RR fruits, total carotenoids were 1.85-fold higher than WT (1.48 fold in *acs2-1*). This increase in *acs2-1* was mainly contributed by a near doubling of lycopene and phytoene. Strikingly, *acs2-2,* and homozygous (*acs2-2*/*acs2-2*) F_2 RR fruits also had higher total carotenoids, mainly due to higher accumulation of lycopene. In the *acs2-2*, levels of different carotenoids at all ripening stages were distinctly different from both WT and *acs2-1* **(Figure 5B)**.

***acs2-1* mutation affects primary metabolites level in fruits**

The ripening of tomato is driven by extensive metabolic shifts making fruits palatable. Several of these metabolic changes are triggered by ethylene, as fruits of *Nr* mutant, which is deficient in ethylene perception, has altered patterns of metabolic shifts than WT (Osorio et al., 2011). Consistent with the major role of ethylene in ripening, PCA revealed distinct differences between metabolites of *acs2-2*, *acs2-1*, and WT fruits at all stages of ripening **(Figure 6A, Supplemental dataset 4)**. The PCA profiles of backcrossed F_2 fruits were distinctly closer to the parental line. The PCA profile of parent *acs2-1* and homozygous mutant (BC_1F_2, *acs2-1*/*acs2-1*) overlapped. Similarly, the PCA profiles of WT parent and homozygous (BC_1F_2, *ACS2-1*/*ACS2-1*) distinctly overlapped at MG and TUR and were in close vicinity at RR. Consistent with the above PCA profiles, the metabolome of BC_1F_2 (*ACS2-1*/*acs2-1*) heterozygous mutant fruits was intermediate between WT and *acs2-1*. The same was reflected in PCA, where heterozygote BC_1F_2 (*ACS2-1*/*acs2-1*) occupied an intermediate position between WT and *acs2-1* **(Figure 6B)**. A similar overlap in PCA profiles was also observed for *acs2-2,* where homozygous mutant (BC_1F_2, *acs2-2*/*acs2-2*) overlapped with respective parent, and heterozygous (BC_1F_2, *ACS2-2*/*acs2-2*) showed intermediate PCA profile **(Figure 6C)**. The above overlaps in PCA profiles of BC_1F_2 plants with respective parental plants indicated that the metabolic shifts were specifically linked with the mutated copies of the respective genes. The intermediate PCA profiles of heterozygous

BC_1F_2 plants indicated a likely semi-dominant influence of *acs2-1* and *acs2-2* mutations on the metabolite level.

The comparison of metabolite profiles of *acs2-1 and acs2-2* (**Figure 7**) and their backcrossed progeny with WT highlighted a strong linkage between the mutated gene and the metabolome. The metabolome of *acs2-1* and of BC_1F_2 *acs2-1/acs2-1* was closer to each other at all stages of ripening than WT. Similarly, the metabolome of WT and BC_1F_2 *ACS2-1/ACS2-1* showed only mild differences. The same was observed for metabolite profiles of *acs2-2* and of BC_1F_2 *acs2-2/acs2-2* fruits (**Figure 7, Supplemental dataset 4**). The metabolome of *ACS2-1/acs2-1* and *ACS2-2/acs2-2* was intermediate, indicating that mutated copy of the respective gene also influenced metabolome in the heterozygous stage. The observed profiles of metabolome were also consistent with the PCA profiles of mutated plants and their backcrossed progeny.

The comparison of metabolite profiles of *acs2-1* and *acs2-2* highlighted distinct differences between the two mutants. The effect of *acs2-1* on the relative up-/down-regulation of most metabolites was milder than *acs2-2* at all stages of fruit ripening. In *acs2-2*, the majority of amino acids derived from the glycolysis pathway were upregulated at most ripening stages, whereas *acs2-1* only mildly affected the aminome except 10-fold higher methionine in RR fruits. Commensurate with high ethylene emission and methionine, ACC levels were also high in *acs2-1* fruits at the RR stage. In *acs2-2*, 2-oxoproline was upregulated at all ripening stages. Similar to the aminome, most organic acids were downregulated in *acs2-1* fruits at all ripening stages. Only a few organic acids were upregulated in *acs2-1*, such as citrate, α-ketoglutaric acid, isocitric acid (TUR, RR), and succinate (TUR). Similarly, only a few organic acids were upregulated in *acs2-2* [Lactate; Oxalate (MG, TUR); Phosphoric acid; Maleate (MG)]. Compared to *acs2-2*, fewer sugars were higher in *acs2-1* than the WT. In *acs2-2*, the sucrose and glucose-6-phosphate were higher than the WT (Supplemental figure 7).

***acs2-1* mutation elevates ETR3/4 expression**

The system II ethylene synthesis in ripening tomato fruits is associated with higher transcript levels of *ACS2*, *ACS4*, *ACO1*, *ACO2* and *ACO3* (Liu et al., 2015). During ripening, the transcript levels of *ACS2*, *ACS4*, *ACO1*, and *ACO2* genes were upregulated in *acs2-1*, in homozygote F_2 (*acs2-1*/*acs2-1*) and in heterozygote F_2 (*ACS2-1*/*acs2-1*) at TUR and RR stages than parental WT and F_2 WT (*ACS2-1*/*ACS2-1*) (**Figure 8A**). Contrastingly, in *acs2-2*, in homozygote F_2 (*acs2-2*/*acs2-2*), and in heterozygote F_2 (*ACS2-2*/*acs2-2*) the transcript levels of

ACS2 (Barring RR in *acs2-2*), *ACS4* (Barring TUR in *acs2-2*), *ACO1*, *ACO2* and *ACO4* (Barring *ACS2-2*/*acs2-2*), genes were lower during ripening WT. Both *acs2-1* and *acs2-2* and their respective homozygous F_2 progeny had no consistent influence on transcript levels of *ACO3*. Out of six *ETR* genes in tomato, *acs2-1* specifically upregulated *ETR3*, *ETR4* at TUR stage **(Figure 8A)**. In contrast, *acs2-2* and its homozygote F_2 (*acs2-2*/*acs2-2*), downregulated *ETR1*, *ETR2*, and *ETR4* (Barring *acs2-2* at BR) at all stages of ripening. For *ETR5*, only homozygote F_2 (*acs2-2*/*acs2-2*) showed downregulation at BR and RR stage. For *ETR6*, no consistent influence of *acs2-1* or *acs2-2* and their homozygote was observed.

We next examined whether the higher carotenoids level in *acs2-1* and *acs2-2* was also associated with increased expression of carotenoid biosynthesis genes. The influence of *acs2-1*, its homozygote F_2 (*acs2-1*/*acs2-1*) and heterozygote F_2 (*ACS2-1*/*acs2-1*) on the expression of carotenoid biosynthesis genes at TUR and RR stages was mainly confined to three genes of pathway- phytoene synthase1 (*PSY1*), phytoene desaturase (*PDS*), and carotenoid isomerase (*CRTISO*). The higher transcript levels of *PSY1*, *PDS* and *CRTISO* in heterozygote F_2 (*ACS2-1*/*acs2-1*) fruits indicate a semi-dominant influence of *acs2-1* on these genes. The *acs2-1* homozygote also upregulated chromoplast-specific lycopene-β-cyclase (*CYCB*). Beside above genes, *acs2-1* upregulated *NCED1* and *ZEP* (Only at TUR) expression. Interestingly, the expression of *PSY1* followed opposing pattern in *acs2-2* with lower transcript levels. Few other genes in *acs2-2* were downregulated at specific stages, viz. *ZDS* (At TUR in homozygote), *CRITSO* (Homo- and hetero-zygote at TUR, Homozygote at RR), and *CYCB* (Homo- and hetero-zygote at RR) **(Figure 8B)**.

1-methylcyclopropene treatment delays on-vine ripening

To ascertain that higher ethylene emission accelerated the ripening of *acs2-1* fruits, we blocked ethylene signal transduction by enclosing MG fruits in sealed bags containing 1-methylcyclopropene (MCP) (**Supplemental Figure 8**). It is believed that MCP noncompetitively blocks ethylene from binding to ethylene receptors (Martínez-Romero et al., 2007**)**. MCP treatment slowed the fruit ripening, delaying the RR stage by 8 days in WT, and 3 days in *acs2-1* **(Supplemental Figure 8)**. Interestingly, the PCA profiles of the MCP-treated *acs2-1* and WT fruits were close at all ripening stages. The above proximity in PCA indicates that, both in WT and *acs2-1*, MCP affected several metabolites levels in identical fashion **(Figure 9A)**. Consistent with this, nearly 45% of metabolites in *acs2-1* and WT were modulated alike by MCP at each stage of

ripening. Almost 22 metabolites, including α-ketoglutaric acid, malic acid, aconitic acid, fructose, mannose, L-cysteine, β-alanine, 5-oxoproline were identically affected in MCP-treated WT and *acs2-1* fruits at all ripening stages **(Figure 9B) (Supplemental dataset 5)**. It appears that notwithstanding the genetic difference between *acs2-1* and WT plants, MCP affects a similar subset of metabolic processes during ripening. Since MCP strongly suppresses the expression of *ETR* genes during tomato fruit ripening (Mata et al., 2018), this similarity may result from the reduction in ETR-mediated signaling in the ripening fruits.

DISCUSSION

Ethylene plays several essential roles throughout the life cycle of plants, regulating a plethora of developmental and stress responses. Among these, ethylene regulation of the ripening of climacteric fruits has drawn the most attention. In this study, the comparison of two contrasting *ACS2* mutants of tomato uncovers that besides regulating fruit ripening; ethylene produced from *ACS2* also modulates several aspects of tomato phenotype right from seed germination.

Ethylene promotes seed germination in tomato

It is established that in the majority of higher plants, the onset of seed germination is antagonistically regulated by ABA and GA (Shu et al., 2016). Our results indicate that in addition to ABA and GA, the endogenous ethylene also participates in seed germination. The faster germination of *acs2-1* seeds is likely related to higher ethylene emission. The slower germination of *acs2-2* seeds associated with reduced ethylene emission is in conformity with the above assumption. Consistent with this, the peak emission of ethylene from *acs2-1* seeds coincides with the completion of seed germination (Lashbrook et al., 1998). Considering that transgenic tomato seeds overexpressing *ERF2* show faster germination (Pirrello et al., 2006), it is likely that higher ethylene emission from *acs2-1* seeds may amplify the ethylene signaling.

Seedlings of *acs2-1* grown in the air do not manifest constitutive triple response alike Arabidopsis *ETO* mutants (Guzman and Ecker, 1990) or tomato *Epi* mutant (Barry et al., 2001). Since inhibitors of ethylene biosynthesis/action do not revert the *Epi* phenotype, the *Epi* probably secondarily affects an ethylene-signaling component (Fujino et al., 1989; Barry et al., 2001). Considering that Arabidopsis *eto2* (*ACS5*) and *eto3* (*ACS9*) seedlings produce 20-90 folds higher ethylene than the wild type, the 3-4 fold higher ethylene emission by *acs2-1* seedlings may not be sufficient to elicit a constitutive triple response (Kieber et al., 1993; Chae et al., 2003). Nevertheless, higher ethylene emission from *acs2-1* seems to be the cause for the shorter hypocotyls in etiolated seedlings than WT. The further shortening of hypocotyls on ethylene exposure likely reflects the combined action of external and internal ethylene produced by the respective seedlings, as the shortening of hypocotyls followed *acs2-1* > WT >*acs2-2*.

Ethylene affects both vegetative and reproductive phenotypes

The contrasting phenotypes of *acs2-1* and *acs2-2* may be related to high and low ethylene emission from the respective plants. Despite higher emission of ethylene from leaves, the *acs2-1* plant phenotype had no resemblance to *35S::ACS2* over-expressing tomato plants showing

epinasty, reduced growth, and higher ethylene emission (Lee et al., 1997). Likewise, the vegetative phenotype of the *acs2-1* was quite distinct from the *Epi* mutant that displays an extremely erect growth habit, severely curled leaves, and thickened stems and petioles. However, the *Epi* effect is restricted to vegetative development (Barry et al., 2001), whereas *acs2-1* affects both vegetative and reproductive phenotypes. It is believed that *Epi* primarily affects a pathway required for normal cell expansion and vegetative growth that, in turn, secondarily influences the ethylene-signaling (Barry et al., 2001).

The contrasting phenotypes of *acs2-1* and *acs2-2*, while emanate from high/low ethylene emission, the modulation of other phytohormones and metabolites levels too underlie phenotypic differences. The hormonal profiling of *acs2-1* and *acs2-2* leaves indicated crosstalk between ethylene and other phytohormones. Consistent with the role of ethylene in regulating leaf senescence in tomato (John et al., 1995), the detached leaves of *acs2-1* showed faster senescence, while senescence of *acs2-2* was slower. Tomato plants cultivated under high salinity while show a positive correlation between ACC level and leaf senescence; the onset and progression of senescence was best correlated with the zeatin/ACC ratio (Ghanem et al., 2008). The opposite levels of zeatin and ethylene in *acs2-2* and *acs2-1* leaves are in conformity with the above notion that ethylene/zeatin ratio is a key determinant regulating leaf senescence. Likewise, high ABA and ethylene levels in *acs2-1* leaves are in conformity with the parallel increase in ABA and ethylene levels in salt-stressed tomato plants (Ghanem et al., 2008; Amjad et al., 2014).

Generally, the plants undergoing pathogen invasions or insect attacks show a concerted action of ethylene with SA and JA to activate the defense responses (Pieterse et al., 2009; Yang et al., 2015). In tomato plants infected with fungal pathogen *Alternaria alternata*, ethylene and JA acted synergistically to promote the susceptibility. Conversely, SA promoted the resistance to the *Alternaria* and antagonized the ethylene signaling (Jia et al., 2013). Therefore, it is conceivable that higher ethylene emission in *acs2-1* affects the levels of other defense hormones such as JA and SA. The upregulation of JA and MeJA and downregulation SA in leaves of *acs2-1* are in conformity with this assumption.

The relationship between auxin and ethylene is complex and shows tissue/organ-specific responses. While ethylene and auxin synergistically regulate root elongation and root hair formation, they antagonistically regulate lateral root formation and hypocotyl elongation (Muday et al., 2012). Auxin and ethylene co-act to regulate tomato root penetration in the soil (Santisree

et al., 2011). Conversely, ACC treatment reduces the free auxin levels in tomato roots indicating antagonistic action of ethylene (Negi et al., 2010). The reduction in IAA and IBA levels in *acs2-1* points toward an antagonistic action of ethylene on the IAA/IBA level. Considering that barring zeatin and SA, the levels of other hormones are not affected in *acs2-2* leaves; it is plausible that hormonal modulation in *acs2-1* leaves may reflect a response analogous to stress, where on surpassing a threshold level, ethylene modulates the levels of stress-related hormones.

The distinct PCA profiles of mutants compared to WT are consistent with contrasting ethylene emission from mutants. The cross-comparison showed that in *acs2-1*, most metabolites were downregulated, while in *acs2-2*, several were upregulated than WT. It is evident that altered ethylene emission from *acs2-1* and *acs2-2* leaves shifts the metabolic profiles in the opposite fashion. The higher level of citrate, isocitrate, and lower level of malate in *acs2-1* leaves indicate an upsurge in respiratory metabolism, a hallmark of stress. It is proposed that the accumulation of citrate is a response mechanism to alleviate stress by induction of alternative oxidase (Gupta et al., 2012). The differences in ethylene emission also influenced the reproductive phenotype, as both mutants display opposite phenotypes for flower numbers and fruit set compared to WT. Taken together, it is implicit that distinct phytohormone and metabolite profiles of the respective mutants underlie the differences in their growth and phenotypes.

acs2-1 fruits show a faster transition to the mature green stage

Several studies have supported the notion that the system-I ethylene emission operates during tomato fruit expansion, while post-MG stage induction of ripening is contributed by system-II ethylene emission (Giovannoni et al., 2017). It is believed that *ACS2* contributes to the system-II ethylene emission, whereas its role in system-I ethylene emission is minimal. Contrary to this, the faster progression to the MG stage in *acs2-1* signifies an additional role for *ACS2* in system-I ethylene emission. Consistent with this, micro-Tom fruits exposed to ethylene too showed faster attainment of the MG stage (Kevany et al., 2007). The fruits of *acs2-1* were smaller, perhaps due to the shorter duration between anthesis and attainment of the MG stage.

Our results support the view that the transition from MG to RR stage is linked with ethylene-induced ripening. Post-MG stage, the faster progression to RR stage and onset of senescence in *acs2-1* is consistent with the pivotal role of ACS2 in the progression of ripening. The above assumption is also corroborated with slower progression to the RR stage and delayed senescence in *acs2-2* fruits. The shorter MG to RR transition period in *acs2-1/acs2-1* and a far-

longer period in *acs2-2/acs2-2* backcrossed progeny further corroborate the close linkage with ACS2. This entails that alleles of *ACS2* can be potentially used for modulating on-vine tomato ripening.

Ethylene also influences the transcript levels of *ETR3*/4 genes

The higher transcript level of *ETR3* and *ETR4* in *acs2-1* fruits at TUR stage indicates likelihood of their stimulation by ethylene (Lashbrook et al., 1998; Kevany et al., 2007). The lowered transcript levels of *ETR1, 2, 4, 5* in *acs2-2* indicates that their expression is also related to ethylene levels ((Okabe et al., 2011; Mubarok et al., 2019). The higher *ACS2, ACS4*, *ACO1* and *ACO2* transcript levels in ripening *acs2-1* fruits is in conformity with the notion that ethylene in an autocatalytic fashion enhances its own synthesis. Consistent with this, reduced ethylene emission from *acs2-2* fruits lowers *ACS2, ACS4*, *ACO1, ACO2,* and *ACO4* transcript levels. Taken together, it appears that higher ethylene emission from *acs2-1* fruits promotes higher transcript levels of ripening-specific ethylene biosynthesis genes and ethylene receptors, and the converse takes place in *acs2-2*.

ACS activity of mutants is related to levels of immunodetectable proteins

The *in vitro* assays corroborated that higher ethylene emission was causally related to ACC synthase activity. In ripening tomato fruits, the endogenous ACC content closely correlates with ethylene emission (Hoffman and Yang, 1980). Higher ethylene emission from *acs2-1* fruits also correlates with higher ACC as well as MACC levels. The *acs2-1* fruits also had higher ACS and ACO enzyme activities. Considering that *acs2-1* fruits accumulate 5-fold higher ACS2 protein, it may have contributed to higher ACS activity. Conversely, lower ethylene emission from *acs2-2* was associated with lower ACC and MACC levels, reduced ACS, and ACO enzyme activities and lower amounts of ACS2 protein.

The large differences in immuno-detectable ACS2 protein in *acs2-1* and *acs2-2* fruits indicated that the above mutations likely affect transcription or stability of the protein. The likelihood of enhanced stability of *ACS2* protein in *acs2-1* by post-translational modification seems to be remote. Typical of type-I ACS, tomato ACS2 protein has three conserved serine phosphorylation sites in C-terminal (Tatsuki and Mori, 2001; Kamiyoshihara et al., 2010). However, there was no difference in phosphorylation magnitude in ACS2 protein in mutants and WT. In Arabidopsis *eto2* (ACS5) and *eto3* (ACS9) mutants encoding Type-II ACS, mutations close to C-terminal stabilizes ACS protein by making it resistant to E3 ligase dependent proteolysis

(Chae and Kieber, 2005). However, Type-I ACS proteins are not subjected to ubiquitin-mediated proteolysis. It remains possible that α-helix change by V352E confers protein stability or stimulates ACS2 catalytic activity. The above possibility is supported by *in silico* analysis showing higher stability for *acs2-1* protein than WT, which may have contributed to increased ACS2 levels in the *acs2-1*.

Notwithstanding, *in silico* prediction of higher protein stability in *acs2-1*, the increased *ACS2* transcript level in *acs2-1* fruit seems to also contribute to the higher amount of ACS2 protein. The abundance of mRNA is governed by a combination of transcription, splicing, and turnover. The A398G mutation in *acs2-1* is located at the 5′ splice site of the second-exon and third-intron junction. The presence of G at the splice junction is predicted to confer more efficient mRNA splicing than WT (http://www.cbs.dtu.dk/services/NetGene2/; Hebsgaard et al., 1996), which in turn may boost *ACS2* transcript levels. A large-scale analysis revealed that synonymous alleles bearing guanine or cytosine at the third position of a codon increased mRNA half-life (Duan et al., 2013). Considering A398G (K=) is a synonymous mutation, it may have enhanced the half-life of *acs2-1* mRNA. During the climacteric phase of tomato ripening, ethylene upregulates *ACS2* transcripts in a positive feedback fashion (Alba et al., 2005; Nakatuska et al., 1998). It is plausible that higher ethylene emission from *acs2-1* fruits in an autocatalytic fashion boosted the *ACS2* transcript levels, which in turn led to a higher level of ACS2 protein. Taken together, the available evidence points that the enhanced transcript levels in the *acs2-1* along with a likely increase in protein stability seem to contribute to the increased ACS2 protein level.

Considering *acs2-2* harbors two mutations in the promoter, the lower level of ACS2 protein seems to be a consequence of reduced *ACS2* transcript level in *acs2-2* fruits. These mutations most likely affect transcript levels of *ACS2* by perturbing interactions between transcription factors (TFs) and their binding sites. Among the transcription factors interacting with mutated sites, AZF is a known repressor of ABA-mediated gene expression (Kodaira et al., 2011). It is plausible that gain of AZF binding site due to T-106A mutation in *acs2-2* promoter may reduce its expression. In addition, mutation at T-382A may hinder demethylation during ripening thus affecting *acs2-2* transcript levels. Anyhow, the contrasting transcript levels, ACS2 protein levels, ACS enzyme activity, and ethylene emission supports the notion that *acs2-1* is a gain-of-function, and *acs2-2* is a loss-of-function mutation.

Ethylene also modulates phytohormones level during ripening

While ethylene is considered as a master regulator of tomato ripening, evidence indicates that other hormones also participate in this process. Auxin appears to act antagonistically to ethylene, as exogenous auxin application delayed the transition from MG to orange/red stage (Su et al., 2015). In tomato, the maximum amount of ABA precedes increased ethylene production in ripening fruits (Zhang et al., 2009). Profiling of phytohormones in the *shr* mutant revealed that hyperaccumulation of NO influenced temporal changes in ethylene, auxins, and ABA during fruit ripening (Bodanapu et al., 2016). Notwithstanding these studies, little information is available about the influence of ethylene on the levels of other phytohormones during ripening. The action of an individual hormone vis-à-vis a combination of multiple hormones is likely to be different. For example, ethylene applied alone stimulates stomatal closure (Desikan et al., 2006), whereas, in concert with other hormones, it opposes stomatal closure (Tanaka et al., 2005, 2006). It entails that though ethylene is a master regulator of ripening, yet it may cross-talk and influence the levels of other hormones during ripening.

Consistent with the above notion, profiling of hormonal levels of tomato fruits revealed that ethylene influences levels of other phytohormones at all stages of ripening. The *acs2-1* fruits displayed higher levels of zeatin, ABA, JA, MeJA, and SA. The downregulation of ABA and SA in *acs2-2* fruits is in conformity with the above view. The higher auxin level in *acs2-2/acs2-2* MG and TUR fruits is consistent with the reported antagonism in auxin and ethylene action during early phase of tomato fruit ripening (Su et al., 2015). Additionally, it is reported that ABA acts as a positive regulator of ethylene biosynthesis at onset of ripening in tomato (Zhang et al., 2009). Our results indicate that ethylene too, acts as a positive regulator of ABA in ripening fruits, as levels of ABA are higher in *acs2-1* and are lower in *acs2-2*. The increase in ABA level is probably mediated by upregulation of *NCED1* expression in *acs2-1*, a gene involved in ABA biosynthesis. Considering that both JA and MeJa levels are higher in *acs2-1* and MeJa levels are lower in *acs2-2/acs-2-2* there seems to be a positive correlation between ethylene and JA levels in tomato fruits. In conformity with this jasmonate deficient tomato mutants show lower ethylene emission during fruit ripening (Liu et al., 2012). The interaction of ethylene with phytohormones also seems to be organ specific, as evident by lower zeatin level in *acs2-1* leaf, whereas fruits have higher zeatin level. Whilst ethylene modulates the hormonal level in ripening fruits, the interrelationship among these hormones is complex and likely involves intersections of various regulatory pathways (Breitel et al., 2016).

ACS2 mutants show high lycopene level in fruits

The onset of fruit-specific carotenogenesis is closely linked with ethylene biosynthesis as antisense suppression of *ACS2* (Theologis et al., 1993) or defect in ethylene perception in *Nr* mutant (Lanahan et al., 1994) inhibits the characteristic red coloration of tomato fruits. Higher carotenoids level in *acs2-1* is consistent with the linkage between ethylene emission and carotenoid accumulation. Analogous to influence on the hormonal level, *acs2-1* in a semi-dominant fashion boosted the carotenoid levels in heterozygous *acs2-1* plants. Ethylene seems to stimulate carotenoid levels in *acs2-1* by upregulating transcripts of *PSY1, PDS,* and *CRTISO,* the key genes regulating phytoene and lycopene biosynthesis. Surprisingly, though most carotenoid intermediates and key genes transcripts such a *PSY1* and *CRTISO* were downregulated in the *acs2-2*, yet it accumulated a higher level of lycopene. In tomato fruits, the carotenoid biosynthesis is geared towards lycopene accumulation, which is sequestered and stored in plastoglobules and lycopene crystals in chromoplasts (Kilambi et al., 2013; Nogueira et al., 2013). It is likely that the prolonged transition period from MG to RR stage in *acs2-2* facilitated continued synthesis and sequestration of lycopene, in turn leading to higher lycopene levels despite having reduced transcript levels of carotenogenic genes.

ACS2 mutants show contrasting effects on metabolite profiles

Consistent with the pleiotropic effect of ethylene in developmental processes, the levels of several primary metabolites in fruits were altered in *acs2-1* and *acs2-2*. The distinctly different PCA profiles of *acs2-1, acs2-2,* and WT are consistent with the view that hormonal signaling perturbation strongly influences the levels of the metabolites (Bastías et al., 2014). Though *acs2-2* and *Nr* mutant are genetically distinct, a comparison of *acs2-2* and *Nr* metabolite profiles (Osorio et al., 2011) showed a similar shift in levels of at least 13 metabolites from MG to RR stage including key TCA cycle constituents such as citric acid, isocitric acid, and malic acid. This entails that above partial similarity on metabolites between *Nr* and *acs2-2* likely emanates from reduced ethylene-mediated signal transduction in respective mutants.

The reduced CO_2 emission from *acs2-2* fruits seems to be linked with reduced ethylene emission (Tigchelaar et al., 1978). The higher levels of amino acids in *acs2-2* may be linked with reduced respiration diverting glycolysis/TCA cycle intermediates to amino acid synthesis. Likewise, reduced ACS2 activity in *acs2-2* likely leads to high 5-oxproline, which is part of the reactions needed to close the methionine salvage cycle in plants (Ellens et al., 2015). The low

levels of 2-ketoglutarate in *acs2-2*, where 5-oxoproline accumulates, and high level in *acs2-1*, where 5-oxoproline does not accumulate, indicates that methionine salvage cycle differently operates in *acs2-1* and *acs2-2* (Ellens et al., 2015), to prevent the accumulation of α-ketoglutaramate, a toxic molecule (Cooper, 2004).

Our study also highlights that perturbation in the function of a single gene distinctly influences a wide range of metabolites. Importantly, the metabolic shifts associated with the respective mutations of *acs2-2* and *acs2-1* is largely retained in the backcrossed homozygous progeny of the mutants. Likewise, in backcrossed homozygous WT, the metabolic profiles revert to the parental WT. The studies on the genetic control of metabolism have underscored QTLs as the major determinants of metabolic shifts and profiles (Fernie and Tohge, 2017). The co-segregation of the metabolite profiles with respective *acs2* gene mutations is in conformity with the above notion. Importantly, it also highlights that an increase/decrease in the ethylene levels in mutants has a cascading effect on plant metabolism, which in turn, accelerates/decelerates the ripening of tomato fruits.

The accelerated ripening of *acs2-1* tomato fruits is in conformity with the notion that higher ethylene emission promotes fruit ripening. Conversely, defect in ethylene perception in tomato *Nr* mutant leads to loss of ripening phenotype (Tieman et al., 2000). The ethylene action can be blocked by MCP, which represses ethylene signaling by binding to ethylene receptors with much higher affinity than ethylene (Sisler et al., 1996; Sisler, 2006). Consequently, MCP exposure to ripening tomato fruits reduces the ethylene emission and downregulates the expression of *ACS2*, *ACS4*, *ACO1* (Yan et al., 2013; Yokotani et al., 2009), *ETR3,* and *ETR4 (*Mata et al., 2018). Consistent with this, MCP application delayed on-vine ripening of both WT and *acs2-1* fruits. The effect of MCP is not restricted to ETRs; it also affects the expression of nearly 65% of ripening-associated genes in tomato (Yan et al., 2013). In conformity with the wide-ranging influence of MCP on ripening-associated genes, the metabolite profiles of treated fruits were distinct from WT and *acs2-1*. Considering that nearly 45% of metabolites in MCP-treated WT and *acs2-1* fruits were identically affected, it can be assumed that this similarity emanated from MCP blockage of ethylene perception in the above fruits.

In conclusion, our results demonstrate that besides the pivotal role in regulating tomato fruit ripening, *ACS2* participates in several facets of tomato development. The faster onset of germination in the *acs2-1* highlights the role of *ACS2* in seed germination. The contrasting

phenotypes of mutants during vegetative and reproductive development, including senescence, are in the conformity of *ACS2* as a key ethylene biosynthesis enzyme during tomato development. The distinct influence of *acs2* mutants on hormonal and primary metabolite profiles of plants also support a tight intertwining of these processes in regulating plant development. The faster transition to the MG stage in the *acs2-1* mutant is suggestive of the role of ethylene in tomato fruit development in addition to the climacteric ripening of tomato fruits. Our results also highlight that the promoter mutations also play an important role in regulating the ethylene level. In the future, the targeted mutagenesis of promoters may become a key tool for modulating the plant developmental responses.

METHODS

Plant material and mutant isolation

Two EMS-mutagenized populations of tomato (*Solanum lycopersicum*) cultivars, M82 (Menda et al., 2004), and Arka Vikas were used for screening of mutants (**Supplemental Table 1**). Genomic DNA was isolated from cotyledons of plants that were 8-fold pooled in two dimensions, as described in Sreelakshmi et al. (2010). The CODDLE software (blocks.fhcrc.org/proweb/coddle) was used for the prediction of the most deleterious regions by mutagenesis. The mutation detection in the population and validation in the progeny was carried out on the LICOR 4300 DNA analyzer using the standard protocol described by TILL et al. (2006) (**Supplemental Table 9)**. The *1-aminocyclopropane-1-carboxylate synthase 2* (*ACS2*) gene sequence (Solyc01g095080.2.1) was obtained from the website of the SOL Genomics Network (https://solgenomics.net/feature/17692657/details). The PCR products were sequenced by Sanger's method by Macrogen Inc. Korea. The sequences were aligned using the MultAlin Interface page (Corpet et al., 1988). The effect of the mutation on protein function was determined by using SIFT (Sorting Intolerant from Tolerant, www.sift.dna.org) software version 4.0.5 (Sim et al., 2012). The presence of mutated gene copy and its zygosity in backcrossed plants was monitored by the CEL-I endonuclease assay (Mohan et al., 2016).

Morphological and biochemical characterization of mutants

The seeds were surface sterilized with 4% (v/v) sodium hypochlorite and after washing were sown on filter papers. The emergence of the radicle was considered as the onset of germination. Seed germination was visually monitored at 12-h intervals. For the seedling phenotype, the sprouted seeds were sown on agar (0.8% w/v), and plates were vertically positioned in light (100 µmol m^{-2} s^{-1}) or darkness. To elicit the ethylene-induced growth inhibition, seedlings were grown in darkness in airtight plastic boxes on agar 0.8% (w/v), and a known volume of ethylene was injected in the box at the onset of the experiment.

The plants were grown in the greenhouse under natural photoperiod (12-14 h day, 28±1°C; 10-12 h night, 14-18°C). The difference between WT and the mutant phenotype was visually monitored and photographed. The leaves were harvested from the seventh node of 45-day-old plants for senescence, pigments, hormonal levels, and ethylene emission studies. The floral and inflorescence morphology were from the second and third truss. For leaf senescence study, the leaves were laid on moist filter papers in Petri plates kept under white light (100 µmole m^{-2} s^{-1}),

and in darkness. The chlorophyll level was determined after 80% acetone (v/v) extraction and centrifugation using the formula of Arnon (1949). The carotenoids level was determined by following the protocol of Gupta et al. (2015).

Estimation of ethylene and CO_2 emission

The ethylene emission was monitored using a previously described procedure (Kilambi et al., 2013). The seedlings were transferred to an airtight glass vial on 0.8% (w/v) agar for 24 h. For leaves, the detached leaves were placed on moistened filter paper and enclosed in airtight petriplates for 4 h. For ethylene emission from fruits, the WT and mutant fruits at different ripening stages (MG: mature green, TUR: turning, and RR: red ripe) were harvested from the second truss. The fruits were placed in an airtight container for 4 h. At the end of the above-mentioned periods, one mL of headspace was withdrawn from the respective containers to estimate ethylene. For CO_2 emission, the fruits were enclosed in a closed chamber containing the CO_2 sensor (Vernier Carbon Dioxide Gas Sensor, CO_2-BTA) for 10 min. Thereafter, the CO_2 emission was monitored using preinstalled Graphical Analysis^{TM} 4 software.

On vine studies

The fruit development was monitored on the vine from the day post-anthesis (DPA) through different stages of ripening (MG, TUR, and RR) until the fruit skin wrinkled. The transition to different ripening stages was visually monitored by fruit color changes. The fruits were photographed from the mature-green or red stage onwards. The firmness of detached fruits, pH, and °Brix was measured as described in Gupta et al., (2014). The diameter of developing fruits of WT and mutants was recorded using a digital Vernier caliper ($n \geq 5 \pm$ SE).

Estimation of ACC levels, ACS and ACO activity

The 1-aminocyclopropane-1-carboxylic acid (ACC) levels, malonyl-ACC (MACC) levels, ACS activity, and ACO activity, were estimated in WT and mutant fruits using the protocol described by Bulens et al., (2011). For ACC estimation, the fruit tissues were homogenized in the presence of 5% (w/v) sulphosalicylic acid, followed by the addition of 10 mM $HgCl_2$ and release of ethylene by the addition of 4% (w/v) NaOCl and saturated NaOH (2:1, v/v). One mL of headspace was withdrawn for ethylene estimation. For calculation of total ACC, acid hydrolysis of the extract was performed. The ACC and MACC amounts were calculated based on the total amount of ethylene released from the unspiked-sample and ACC-spiked sample using the formula given by Bulens et al. (2011).

To determine ACS activity, 1 g of fruit tissue was homogenized in liquid N_2 and mixed with the extraction buffer by vortexing. The supernatant obtained after centrifugation (21,000*g*) was desalted on Sephadex G25 column. The eluted fraction was assayed for ACS activity in a reaction mixture containing s-adenosine methionine (SAM) in a closed vial. The reaction was terminated by adding $HgCl_2$, and ethylene was released by adding NaOCl/NaOH mixture. One mL of headspace was withdrawn for ethylene estimation. For ACO activity, 500 mg of fruit tissue was homogenized in liquid N_2 and mixed with the extraction buffer by vortexing. After centrifugation, the ACO activity was estimated in a reaction mixture containing 1 mM ACC in a closed vial. After 15 minutes of incubation, one mL headspace sample was withdrawn for ethylene estimation. The ACS and ACO activity was calculated using the formula given by Bulens et al. (2011).

Immunodetection of ACS protein levels

The polyclonal antibodies were raised in rabbits against ACS2 protein using a peptide "EHGENSPYFDGWKAYDSD" custom synthesized by PEPTIDE 2.0, USA. The Ig fraction was purified using DEAE-Sepharose column using standard protocols. The fruits were homogenized in Tricine buffer (200 mM, pH 8.5), 2 mM pyridoxal-5-phosphate (PLP, 10 mM DTT (Dithiothreitol) with 50 mg PVPP. The homogenate was centrifuged (21,000*g* for 30 min at 4°C) and the supernatant was desalted on Sephadex G25 column. The eluted sample was immunoprecipitated after the estimation of protein using Bradford's (1976) assay. The supernatant was gently shaken with purified IgG fraction at 37°C for 1 h, followed by 1 h shaking with protein-A Sepharose at 4°C. The beads were recovered by centrifugation (12,000*g* at 4°C for 30 min). The supernatants were analyzed for the reduction in ACS2 activity, and protein-A Sepharose beads were used for western blotting.

The immunoprecipitated ACS2 protein was recovered by boiling in SDS-PAGE loading buffer and separated in 12% gel following the protocol of Laemmli (1970). The gel was electroblotted on the PVDF membrane using semi-dry blotting followed by Western blotting, as described by Towbin et al. (1979). The non-specific binding sites on the membrane were blocked by incubating with milk powder. The membrane was first incubated with ACS-antibody (1/1500 dilution), followed by incubation with an anti-rabbit IgG goat antibody (1/80,000 dilution), coupled with alkaline phosphatase. The alkaline phosphatase activity was visualized by using standard BCIP-NBT staining assay.

Profiling of phytohormones, carotenoids, and metabolites

The phytohormone levels were determined from leaves from the 7th node of 45-day-old plants and fruits using Orbitrap Exactive-plus LC-MS following the protocol described earlier (Pan et al.,2010; Bodanapu et al., 2016). Carotenoid profiling was carried out following the procedure of Gupta et al. (2015). Metabolite analysis by GC-MS was carried out by a method modified from Roessner et al. (2000) described in Bodanapu et al. (2016). The metabolite identification was carried out with the NIST (National Institute of Standards and Technology) GC/MS Metabolomics library software (NIST/EPA/NIH Mass Spectral Library 14, Department of Commerce, USA). Statistical analysis and PCA was done using MetaboAnalyst 4.0, a web-based suite for high-throughput metabolomic data analysis (Xia et al., 2012).

RNA isolation and Quantitative Real-time PCR

The RNA was isolated from the pericarp of fruits using TRI reagent (Sigma, USA). The isolated RNA was treated with RQ1 RNase Free DNase (Promega) to remove DNA. Reverse transcription was performed with 2 µg RNA using the Affinity Script QPCR cDNA Synthesis Kit (Agilent Technologies). All the above steps were carried out following the respective manufacturer's protocol. Quantitative real-time PCR was performed with about 4 ng of total RNA in a 10-µL reaction volume using iTaq Universal SYBR green Supermix (BIORAD) on an AriaMx Real-time PCR system (Agilent technologies). Gene-specific primers were designed from the sequences obtained from Solanaceae Genomics Network the https://solgenomics.net) database using Primer 3 software (**Supplemental Table 10)**. The relative fold differences were determined by normalizing cycle threshold (Ct) values of each gene to the mean expression of both *β-Actin* and *Ubiquitin* genes and were calibrated using the equation $2^{-\Delta Ct}$. Three independent biological replicates were used for each experiment.

On-vine Treatment of fruits with 1-MCP

The dose of 1-methylcyclopropene (MCP) used was standardized by serial dilutions. MCP treatment was given to the fruits of the second truss of the WT and *acs2-1* mutant. The MG fruits were enclosed with ZIP-lock transparent bag containing MCP (200 mg/5 mL water). The fruits were visually observed for the progression of the ripening and were harvested at turning and red stages. The primary metabolite levels were estimated as described in an earlier section.

***In silico* characterization of tomato *ACS2* mutants**

The target protein structure and FASTA sequence of 1-aminocyclopropane-1-carboxylate (ACC) synthase (PDB ID: 1IAX) (Huai et al., 2001) (https://www.rcsb.org/structure/1IAX), having the resolution of 2.8 Å, was retrieved from protein data bank (http://www.rcsb.org/pdb/). The 3-dimensional structure of mutant *ACS2-1* (V352E) and WT proteins were visualized using PyMol (http://www.pymol.org). The prediction of protein 3D stabilization of *ACS2-1* versus WT was computationally analyzed using the following softwares CUPSAT (http://cupsat.tu-bs.de/), MAESTROWeb (https://pbwww.che.sbg.ac.at/maestro/web), PoPMuSiCv3.1 (https://soft.dezyme.com/query/create/pop), STRUM (https://zhanglab.ccmb.med.umich.edu/STRUM/), and DynaMut (http://biosig.unimelb.edu.au/dynamut/).

Splice site analysis of the *acs2-1* mutant was conducted using the NetGene2 server (http://www.cbs.dtu.dk/services/NetGene2/). Promoter sequence analysis of WT and *acs2-2* was performed using the PC base (http://pcbase.itps.ncku.edu.tw/) and also manually for ripening-specific transcription factors.

7.15 Statistical analysis

All results are expressed as mean value ± SE of three or more independent replicates. A Student`s *t*-test was used to determine the significant differences ($P \leq 0.05$) between treatment and control and/or WT and the mutants. The StatisticalAnalysisOnMicrosoft-Excel software (http://prime.psc.riken.jp-/MetabolomicsSoftware/StatisticalAnalysisOn-MicrosoftExcel/) was used to obtain significant differences between data points. Heat maps and clustered heat maps were prepared using publically available Morpheus software (https://software.broadinstitute.org/morpheus/). 3D PCA plots were generated using publically available MetaboAnalyst 4.0 software (https://www.metaboanalyst.ca/). Unless otherwise mentioned, the statistical significance (*, #, $) marked in all figures was determined using Student's t-test. (* for $P \leq 0.05$, # for $P \leq 0.01$ and $ for $P \leq 0.001$).

Supplemental Data

Supplemental Figure 1. Prediction of deleterious mutation susceptible region in the *ACS2* gene by CODDLE software.

Supplemental Figure 2. Splice site analysis of *acs2-1* mutant by NetGene2 server.

Supplemental Figure 3. Chlorophyll, carotenoids, and xanthophylls levels in the leaf of WT, *acs2-1*, and *acs2-2* mutant.

Supplemental Figure 4. Fruit firmness, total soluble solids (Brix) and pH of WT, *acs2* mutants, and their BC_1F_2 progenies at different ripening stages

Supplemental Figure 5. Raising and validation of antibodies specific for ACS2 peptides.

Supplemental Figure 6. Immunoprecipitation and Western blotting of ACS2 protein using purified IgG fraction.

Supplemental Figure 7. The metabolic shifts in *acs2* mutant fruits during ripening in comparison to WT.

Supplemental Figure 8. On-vine treatment of MCP to mature green fruits of WT and *acs2-1* mutant.

Supplemental Table 1. EMS-mutagenized tomato populations used for the isolation of *ACS2* mutants.

Supplemental Table 2. *ACS2* mutant lines identified and confirmed for mutation**.**

Supplemental Table 3. The genetic segregation of *acs2-1* and *acs2-2* mutants in BC_1F_2 generation.

Supplemental Table 4. Increases in ACS2-1 protein stability predicted by different software.

Supplemental Table 5. The alteration of bonding pattern in ACS2 protein in *acs2-1* mutant compared to WT protein.

Supplemental Table 6. Disruption in transcription factor binding site in *acs2-2* due to promoter mutation.

Supplemental Table 7. Changes in methylation status of *ACS2* promoter at -106 and -382 position during fruit ripening.

Supplemental Table 8. Comparisons of flower numbers and fruit set in WT and *acs2* mutants**.**

Supplemental Table 9. List of primers used for screening for mutations in *ACS2* by TILLING

Supplemental Table 10. List of genes and the primers used for qRT-PCR analysis.

Supplemental dataset 1. The transcription factor binding sites in the *ACS2* and *acs2-2* promoter predicted by Plant ChIP-seq Database.

Supplemental dataset 2. Changes in methylation status of *ACS2* promoter during fruit ripening.

Supplemental dataset 3. List of metabolites identified in leaves of WT and *acs2* mutants.

Supplemental dataset 4. List of metabolites identified at different fruit ripening stages of WT and *acs2* mutants.

Supplemental dataset 5. List of metabolites identified in MCP-treated WT and *acs2-1* fruits.

AUTHOR CONTRIBUTIONS

R.S and Y.S. designed this project and wrote the manuscript. K.S. performed most of the experiments. S.G. isolated mutants using TILLING. S.S. extracted the RNA and did qRT-PCR. M.R. did *in silico* analyses.

ACKNOWLEDGMENTS

We thank Dr. Dani Zamir for providing us EMS-mutagenized M82 cultivar lines of tomato. We thank Dr. Alok Sinha for providing Phospho-Ser antibody. This work was supported by the Department of Biotechnology (DBT), India grants (BT/PR/5275/AGR/16/465/2004, BT/PR11671/PBD/16/828/2008, BT/PR/7002/PBD/16/1009/2012, and BT/COE/34/SP15209/2015) to R.S. and Y.S., DBT post-doctoral research fellowship to S.S., Department of Science and Technology, India, Young Scientist grant to S.G., University Grants Commission, India, Research Fellowship to K.S.

FIGURES LEGENDS

Figure 1. Characterization of *acs2* mutants.

(A) Localization of mutations in the *ACS2* gene in *acs2-1* and *acs2-2*. Arrows indicate the base changes in the introns, exons, splice site, and promoter.

(**B)** Model of ACS2 protein comprising of A and B chains. The altered intermolecular bonding in the respective chain of ACS2 protein due to V352E mutation in *acs2-1* is depicted in the side panels (Red arrows).

(C) Time course of mutant and WT seed germination (n = 30 ± SE).

(D) Time course of ethylene emission from dark-grown *acs2* mutants and WT seedlings. At different time points from sowing, seedlings were transferred to an airtight vial for 24 h for estimation of ethylene.

(E, F) Effect of exogenous ethylene on the root (**E**) and hypocotyl elongation (**F**) of 5-day-old dark-grown seedlings.

Unless otherwise mentioned, the statistical significance marked in all figures was determined using Student's *t*-test. (* for $P \leq 0.05$, # for $P \leq 0.01$ and $ for $P \leq 0.001$).

Figure 2. Characterization of *acs2* mutants and WT plants.

(A, B) Phenotypes of greenhouse-grown WT and *acs2-1* (**A**) and *acs2-2* (**B**) plants.

(**C**) Ethylene emission from leaves of WT and *acs2* mutants.

(**D**) Senescence of detached leaves of WT and *acs2* mutants incubated in darkness or under the light.

(E, F) Phytohormones profiles of WT and *acs2* mutants leaves.

(**G)** Principal component analysis (PCA) of WT and *acs2* mutants (n = 5). The PCA was plotted using the MetaboAnalyst 4.0.

(**H)** Heat maps showing significantly up- or down-regulated (> 1.5 fold) metabolites in *acs2* mutants with reference to WT. The relative changes between mutant and WT were calculated by determining the mutant/WT ratio for individual metabolites.

The leaves harvested from the seventh node of 45-day-old plants were used for all analyses.

Figure 3. The development and on-vine ripening of *acs2* mutants and WT fruits.

(**A**) WT and *acs2* mutant fruits (WT: 39 DPA, *acs2-1*: 30 DPA, *acs2-2*: 40 DPA).

(**B**) Time course of the increase in fruit diameter from anthesis until 45 days. Arrows mark the attainment of the MG stage (n = 3).

(**C**) Chronological development of tomato fruits post-anthesis until the onset of senescence. The stacked bar graph shows the attainment of different stages of ripening: mature green (MG), breaker (BR), Turning (TUR), Pink (P), and red ripe (RR) stages until senescence onset. The time point to attain specific ripening phases was visually monitored. The appearance of wrinkles on fruit skin was taken as time point of senescence onset (WT- 82 DPA; *acs2-1* - 42 DPA; *acs2-1*/*acs2-1* - 44 DPA; acs2-*2*- 102 DPA; *acs2-2*/*acs2-2*-112 DPA)

(**D**) On-vine ripening of second truss WT and *acs2* mutant fruits from RR until senescence onset (Arrowheads).

(E) Ethylene emission from MG, TUR, and RR fruits of WT, *acs2* mutants, and their respective backcrossed homozygous progeny (*acs2-1*/*acs2-1; acs2-2*/*acs2-2*).

(**F**) The CO_2 emission from MG, TUR, and RR fruits of WT and mutants.

Figure 4. ACS activity and protein levels in mutants and WT fruits.

(A, B) ACC (**A**) and MACC (**B**) levels in WT and *acs2* mutants.

(**C, D**) ACS (**C**) and ACO (**D**) enzyme activities in WT and *acs2* mutants.

(**E, F)** Comparison of ACS2 protein levels in RR fruits of WT, *acs2-1* (**E**), and *acs2-2* (**F**) using Western blotting. A similar amount of immunoprecipitated proteins from WT and *ACS2* mutants was serially diluted. Dilutions demonstrate that the abundance of ACS2 protein in *acs2-1* is 4-fold higher, and in *acs2-2*, it is 4-fold lower compared to WT.

(**G**) The equal amount of ACS2 protein (Calculated based on data in **E** and **F**) loaded on Western blot shows similar staining with the Phospho-Ser antibody.

M represents the protein marker

Figure 5. Phytohormones and carotenoids levels during ripening in WT, *acs2* mutants, and their BC_1F_2 progenies.

(**A**) Phytohormones

(**B**) Carotenoids.

The levels of phytohormones were estimated using Liquid Chromatography-Mass Spectrometry (LC-MS). ABA (Abscisic acid), SA (Salicylic acid), IAA (Indole-3-acetic acid), JA (Jasmonic

acid), MeJA (Methyl Jasmonic acid). The carotenoid levels were estimated using UPLC. The BC_1F_2 progenies mentioned in this and following figures consisted of respective WT, heterozygous mutants, and homozygous mutants (WT- *ACS2-1/ACS2-1*; heterozygous- *ACS2-1*/*acs2-1;* homozygous mutant- *acs2-1*/*acs2-1*; WT- *ACS2-2/ACS2-2*; heterozygous- *ACS2-2*/*acs2-2;* homozygous mutant- *acs2-2*/*acs2-2*.)

Figure 6. PCA of metabolites during ripening in WT, *asc2* mutants, and their BC_1F_2 progenies.
(A) PCA of WT and *acs2* mutants.
(B) PCA of WT, *acs2-1*, and its BC_1F_2 progeny.
(C) PCA of WT, *acs2-2*, and its BC_1F_2 progeny.

Figure 7. Relative levels of metabolites in ripening fruits of WT and mutants.
Heat maps show differential expression of metabolites at different ripening stages in fruits of WT, *acs2-1*, *acs2-2*, and their respective BC_1F_2 progenies.
The relative changes of metabolites represent the mutant/WT ratio, calculated using parental WT used for crosses, at respective ripening stages as the denominator. Only significantly up- or down-regulated metabolites are represented in the heat map (> 1.5 fold). For details of BC_1F_2 progenies, see Figure 5.

Figure 8. Relative expression of transcripts of ethylene receptors, ethylene and carotenoids biosynthesis genes during ripening in WT, *acs2* mutants, and their BC_1F_2 progenies.
ACS- 1-aminocyclopropane carboxylic acid synthase; ACO- 1-aminocyclopropane carboxylic acid oxidase; CRTISO- carotenoid isomerase; *CRTR-B2- β-carotene hydroxylase 2; CYCB - chromoplast specific lycopene β-cyclase*; *DXS- deoxy-xylulose 5-phosphate synthase ETR- ethylene receptor; LCYB1- lycopene β-cyclase 1; LCYE- lycopene ε-cyclase; NCED- 9-cis-epoxycarotenoid dioxygenase 1, PDS- phytoene desaturase*; *PSY1- phytoene synthase 1*; *ZDS- ζ-carotene desaturase; ZEP- zeaxanthin epoxidase; ZISO- ζ-carotene isomerase;* For BC_1F_2 progenies details, see Figure 5.

Figure 9. PCA and metabolites levels in treated or untreated fruits of WT and *acs2-1* with 1-methylcyclopropane (MCP).

(**A**) Principal component analysis.

(**B**) The relative accumulation of metabolites.

The relative accumulation of metabolites were calculated by determining the mutant/WT ratio, using untreated WT at respective ripening stages as the denominator. Only significantly up- or down-regulated metabolites are represented in the heat map (> 1.5 fold).

REFERENCES

Abeles FB, Morgan PW, Saltveit Jr ME. (1992) Ethylene in plant biology. Academic press

Adams DO, Yang SF. (1979) Ethylene biosynthesis: identification of 1-aminocyclopropane-1-carboxylic acid as an intermediate in the conversion of methionine to ethylene. *Proc. Natl. Acad. Sci. USA.* **76**: 170-174.

Alba R, Payton P, Fei Z, McQuinn R, Debbie P, Martin GB, Tanksley SD, Giovannoni JJ. (2005) Transcriptome and selected metabolite analyses reveal multiple points of ethylene control during tomato fruit development. *Plant Cell.* **17**: 2954-2965.

Amjad M, Akhtar J, Anwar-ul-Haq M, Yang A, Akhtar SS, Jacobsen SE. (2014) Integrating role of ethylene and ABA in tomato plants adaptation to salt stress. *Sci. Hort.* **172**: 109-116.

Arnon DI. (1949) Copper enzymes in isolated chloroplasts. Polyphenoloxidase in Beta vulgaris. *Plant Physiol.* **24**: 1-15.

Barry CS. (2014) Ripening mutants. *In* "Fruit Ripening: Physiology, Signalling and Genomics" Eds. Nath P, Bouzayen M, Mattoo AK, Pech JC, CABI; pp 246-258

Barry CS, Blume B, Bouzayen M, Cooper W, Hamilton AJ, Grierson D. (1996) Differential expression of the 1-aminocyclopropane-1-carboxylate oxidase gene family of tomato. *Plant J.* **9**: 525-535.

Barry CS, Fox EA, Yen HC, Lee S, Ying TJ, Grierson D, Giovannoni JJ. (2001) Analysis of the Ethylene Response in the epinastic Mutant of Tomato. *Plant Physiol.***127**: 58-66.

Barry CS, Llop-Tous MI, Grierson D. (2000) The regulation of 1-aminocyclopropane-1-carboxylic acid synthase gene expression during the transition from system-1 to system-2 ethylene synthesis in tomato. *Plant Physiol.* **123**: 979-986.

Bastías A, Yañez M, Osorio S, Arbona V, Gómez-Cadenas A, Fernie AR, Casaretto JA. (2014) The transcription factor AREB1 regulates primary metabolic pathways in tomato fruits. *J. Exp. Bot.* **65**: 2351-2363.

Bleecker AB, Kenyon WH, Somerville SC, Kende H. (1986) Use of monoclonal antibodies in the purification and characterization of 1-aminocyclopropane-1-carboxylic acid synthase, an enzyme in ethylene biosynthesis. *Proc. Natl. Acad. Sci. USA* **83:** 7755–7759.

Bodanapu R, Gupta SK, Basha PO, Sakthivel K, Sadhna, Sreelakshmi Y, Sharma R. (2016) Nitric oxide overproduction in tomato *shr* mutant shifts metabolic profiles and suppresses fruit growth and ripening. *Front. Plant Sci.* **7**: 1714

Bradford MM. (1976) A rapid and sensitive method for the quantitation of microgram quantities of protein utilizing the principle of protein-dye binding. *Anal. Biochem.* **72**: 248-254.

Brady CJ. (1987) Fruit ripening. *Annu. Rev. Plant Physiol.* **38**: 155-178

Breitel DA, Chappell-Maor L, Meir S, Panizel I, Puig CP, Hao Y, Yifhar T, Yasuor H, Zouine M, Bouzayen M, Richart AG, Rogachev I, Aharoni A. (2016) AUXIN RESPONSE FACTOR 2 intersects hormonal signals in the regulation of tomato fruit ripening. *PLoS Genet.* **12(3):** e1005903.

Bulens I, Van de Poel B, Hertog ML, De Proft MP, Geeraerd AH, Nicolaï BM. (2011) Protocol: an updated integrated methodology for analysis of metabolites and enzyme activities of ethylene biosynthesis. *Plant Methods.* **7**: 17.

Chae HS, Faure F, Kieber JJ. (2003) The eto1, eto2, and eto3 mutations and cytokinin treatment increase ethylene biosynthesis in Arabidopsis by increasing the stability of ACS protein. *Plant Cell.* **15**: 545-559.

Chae HS, Kieber JJ. (2005) Eto Brute? Role of ACS turnover in regulating ethylene biosynthesis. *Trends Plant Sci.* **10**: 291-296.

Chen G, Alexander L, Grierson D. (2004). Constitutive expression of EIL-like transcription factor partially restores ripening in the ethylene-insensitive Nr tomato mutant. *J. Exp. Bot.* **55:** 1491–1497.

Cooper AJ. (2004) The role of glutamine transaminase K (GTK) in sulfur and alpha-keto acid metabolism in the brain, and in the possible bioactivation of neurotoxicants. *Neurochem. Int.* 44, 557–577.

Corpet F, Gouzy J, Kahn D. (1998) The ProDom database of protein domain families. *Nucleic Acids Res.*. **26**: 323-326.

Desikan R, Last K, Harrett-Williams R, Tagliavia C, Harter K, Hooley R, Hancock JT, Neill SJ. (2006) Ethylene-induced stomatal closure in Arabidopsis occurs via AtrbohF-mediated hydrogen peroxide synthesis. *Plant J.* **47**: 907-916.

Duan J, Shi J, Ge X, Dölken L, Moy W, He D, Shi S, Sanders AR, Ross J, Gejman PV. (2013) Genome-wide survey of inter-individual differences of RNA stability in human lymphoblastoid cell lines. *Sci. Rep.* **20:** 1318

Ellens KW, Richardson LG, Frelin O, Collins J, Ribeiro CL, Hsieh YF, Mullen RT, Hanson AD. (2015) Evidence that glutamine transaminase and omega-amidase potentially act in

tandem to close the methionine salvage cycle in bacteria and plants. *Phytochem.* **113**: 160-169.

Fernie AR, Tohge T. (2017) The genetics of plant metabolism. *Annu. Rev. Genet.* **51**: 287-310.

Fujino DW, Burger DW, Bradford KJ. (1989) Ineffectiveness of ethylene biosynthetic and action inhibitors in phenotypically reverting the Epinastic mutant of Tomato (Lycopersicon esculentum mill.). *J. Plant Growth Regul.* **8**: 53-61.

Fujisawa M, Nakano T, Shima Y, Ito Y. (2013) A large-scale identification of direct targets of the tomato MADS box transcription factor RIPENING INHIBITOR reveals the regulation of fruit ripening. *Plant Cell.* **25**: 371-386.

Fujisawa M, Shima Y, Higuchi N, Nakano T, Koyama Y, Kasumi T, Ito Y. (2012) Direct targets of the tomato-ripening regulator RIN identified by transcriptome and chromatin immunoprecipitation analyses. *Planta*. **235**: 1107-1122.

Gallie DR. (2010) Regulated ethylene insensitivity through the inducible expression of the Arabidopsis etr1-1 mutant ethylene receptor in tomato. *Plant Physiol.***152**: 1928-1939.

Gao Y, Zhu N, Zhu X, Wu M, Jiang CZ, Grierson D, Luo Y, Shen W, Zhong S, Fu DQ, Qu G. (2019) Diversity and redundancy of the ripening regulatory networks revealed by the fruitENCODE and the new CRISPR/Cas9 CNR and NOR mutants. *Hortic. Res.* **6**: 39

Ghanem ME, Albacete A, Martínez-Andújar C, Acosta M, Romero-Aranda R, Dodd IC, Lutts S, Pérez-Alfocea F. (2008) Hormonal changes during salinity-induced leaf senescence in tomato (Solanum lycopersicum L.). *J. Exp. Bot.* **59**: 3039-3050.

Giovannoni J, Nguyen C, Ampofo B, Zhong S, Fei Z. (2017) The epigenome and transcriptional dynamics of fruit ripening. *Annu. Rev. Plant Biol.* **68**: 61-84.

Grierson D. (2013) Ethylene and the Control of Fruit Ripening. *In* The Molecular Biology and Biochemistry of Fruit Ripening. Eds Seymour GB, Tucker GA, Poole M, Giovannoni, J. Wiley-Blackwell Chichester. pp 43-74

Gupta KJ, Shah JK, Brotman Y, Jahnke K, Willmitzer L, Kaiser WM, Bauwe H, Igamberdiev AU. (2012) Inhibition of aconitase by nitric oxide leads to induction of the alternative oxidase and to a shift of metabolism towards biosynthesis of amino acids. *J. Exp. Bot.* **63**: 1773-1784.

Gupta P, Sreelakshmi Y, Sharma R. (2015) A rapid and sensitive method for determination of carotenoids in plant tissues by high performance liquid chromatography. *Plant Methods.* **11**: 5

Gupta SK, Sharma S, Santisree P, Kilambi HV, Appenroth K, Sreelakshmi Y, Sharma R. (2014) Complex and shifting interactions of phytochromes regulate fruit development in tomato. *Plant Cell Environ.* **37:** 1688-1702

Guzman P, Ecker JR. (1990) Exploiting the triple response of Arabidopsis to identify ethylene-related mutants. *Plant Cell*. **2**: 513-523.

Hackett RM, Ho C-W, Lin Z, Foote HCC, Fray RG, Grierson D. (2000) Antisense inhibition of the Nr gene restores normal ripening to the tomato Never-ripe mutant, consistent with the ethylene receptor-inhibition model. *Plant Physiol.* **124**: 1079-1086.

Hamilton AJ, Lycett GW, Grierson D. (1990). Antisense gene that inhibits synthesis of the hormone ethylene in transgenic plants. *Nature* **346***:* 284–287.

Hebsgaard SM, Korning PG, Tolstrup N, Engelbrecht J, Rouze P, Brunak S. (1996) Splice site prediction in Arabidopsis thaliana DNA by combining local and global sequence information, *Nucleic Acids Res.* **24**: 3439-3452

Hoffman NE, Yang SF, McKeon T. (1982) Identification of 1-(malonylamino) cyclopropane-1-carboxylic acid as a major conjugate of 1-aminocyclopropane-1-carboxylic acid, an ethylene precursor in higher plants. *Biochem. Bioph. Res. Co.* **104**: 765–770.

Hoffman NE, Yang SF. (1980) Changes of 1-aminocyclopropane-1-carboxylic acid content in ripening fruits in relation to their ethylene production rates. *J. Am. Soc. Hortic. Sci*. **105**: 492-495.

Huai Q, Xia Y, Chen Y, Callahan B, Li N, Ke H. (2001) Crystal structures of 1-aminocyclopropane-1-carboxylate (ACC) synthase in complex with amino ethoxy-vinylglycine and pyridoxal-5′-phosphate provide new insight into catalytic mechanisms. *J. Biol. Chem.* **276:** 38210-38216

Hunt RC, Simhadri VL, Iandoli M, Sauna ZE, Kimchi-Sarfaty C. (2014) Exposing synonymous mutations. *Trends Genet.* **30**: 308-321.

Itkin M, Seybold H, Breitel D, Rogachev I, Meir S, Aharoni A. (2009) TOMATO AGAMOUS-LIKE 1 is a component of the fruit ripening regulatory network. *Plant J.* **60**: 1081-1095.

Ito Y, Kitagawa M, Ihashi N, Yabe K, Kimbara J, Yasuda J, Ito H, Inakuma T, Hiroi S, Kasumi T. (2008) DNA-binding specificity, transcriptional activation potential, and the rin mutation effect for the tomato fruit-ripening regulator RIN. *Plant J.* **55**: 212-223.

Jia C, Zhang L, Liu L, Wang J, Li C, Wang Q. (2013) Multiple phytohormone signalling pathways modulate susceptibility of tomato plants to *Alternaria alternata* f. sp. *lycopersici*. *J. Exp. Bot.* **64**: 637-650.

John I, Drake R, Farrell A, Cooper W, Lee P, Horton P, Grierson D. (1995) Delayed leaf senescence in ethylene-deficient ACC-oxidase antisense tomato plants: molecular and physiological analysis. *Plant J.* **7**: 483-490.

Kamiyoshihara Y, Iwata M, Fukaya T, Tatsuki M, Mori H. (2010) Turnover of *LeACS2*, a wound inducible 1-aminocyclopropane-1-carboxylic acid synthase in tomato, is regulated by phosphorylation/dephosphorylation. *Plant J.* **64**, 140–150.

Kamiyoshihara Y, Tieman DM, Huber DJ, Klee HJ. (2012) Ligand-induced alterations in the phosphorylation state of ethylene receptors in tomato fruit. *Plant Physiol.* **160**: 488-497

Karlova R, Rosin FM, Busscher-Lange J, Parapunova V, Do PT, Fernie AR, Fraser PD, Baxter C, Angenent GC, de Maagd RA. (2011) Transcriptome and metabolite profiling show that APETALA2a is a major regulator of tomato fruit ripening. *Plant Cell*. **23**: 923-941.

Katz YS, Galili G, Amir R. (20060 Regulatory role of cystathionine-γ-synthase and de novo synthesis of methionine in ethylene production during tomato fruit ripening. *Plant Mol. Biol*. **61**: 255–268.

Kevany BM, Tieman DM, Taylor MG, Cin VD, Klee HJ. (2007) Ethylene receptor degradation controls the timing of ripening in tomato fruit. *Plant J.* **51**: 458-467.

Kieber JJ, Rothenberg M, Roman G, Feldmann KA, Ecker JR. (1993). CTR1, a negative regulator of the ethylene response pathway in Arabidopsis, encodes a member of the raf family of protein kinases. *Cell* **72**: 427-441.

Kilambi HV, Kumar R, Sharma R, Sreelakshmi Y. (2013) Chromoplast-specific carotenoid-associated protein appears to be important for enhanced accumulation of carotenoids in *hp1* tomato fruits. *Plant Physiol.* **161:** 2085-2101

Klee HJ, Giovannoni JJ. (2011) Genetics and control of tomato fruit ripening and quality attributes. *Annu. Rev. Genet.* **45**: 41-59.

Kodaira KS, Qin F, Tran LS, Maruyama K, Kidokoro S, Fujita Y, Shinozaki K, Yamaguchi-Shinozaki K. (2011) Arabidopsis Cys2/His2 zinc-finger proteins AZF1 and AZF2 negatively regulate abscisic acid-repressive and auxin-inducible genes under abiotic stress conditions. *Plant Physiol.* **157**: 742-756

Kudla G, Murray AW, Tollervey D, Plotkin JB. (2009) Coding-sequence determinants of gene expression in Escherichia coli. *Science* **324:** 255–258

Laemmli UK. (1970) Cleavage of structural proteins during the assembly of the head of bacteriophage T4. *Nature*. **227**: 680-685.

Lanahan MB, Yen HC, Giovannoni JJ, Klee HJ. (1994) The never ripe mutation blocks ethylene perception in tomato. *Plant Cell* **6**: 521-530.

Lashbrook CC, Tieman DM, Klee HJ. (1998) Differential regulation of the tomato ETR gene family throughout plant development. *Plant J.* **15**: 243-252.

Lee KY, Baden C, Howie WJ, Bedbrook J, Dunsmuir P. (1997) Post-transcriptional gene silencing of ACC synthase in tomato results from cytoplasmic RNA degradation. *Plant J.* **12**: 1127-1137.

Lin Z, Hong Y, Yin M, Li C, Zhang K, Grierson D. (2008) A tomato HD-Zip homeobox protein, LeHB-1, plays an important role in floral organogenesis and ripening. *Plant J.* **55**: 301-310.

Lin Z, Zhong S, Grierson D. (2009) Recent advances in ethylene research. *J. Exp. Bot*. **60**: 3311-3336.

Lincoln JE, Fischer RL. (1988) Regulation of gene expression by ethylene in wild-type and rin tomato (Lycopersicon esculentum) fruit. *Plant Physiol.* **88**: 370-374

Liu L, Wei J, Zhang M, Zhang L, Li C, Wang Q. (2012) Ethylene independent induction of lycopene biosynthesis in tomato fruits by jasmonates. *J. Exp. Bot.* **63**: 5751–5761

Liu M, Pirrello J, Chervin C, Roustan JP, Bouzayen M. (2015) Ethylene control of fruit ripening: revisiting the complex network of transcriptional regulation. *Plant Physiol.* **169**: 2380-2390

Martel C, Vrebalov J, Tafelmeyer P, Giovannoni JJ. (2011) The tomato MADS-box transcription factor RIPENING INHIBITOR interacts with promoters involved in numerous ripening processes in a COLORLESS NONRIPENING-dependent manner. *Plant Physiol.* **157**: 1568-1579.

Martínez-Romero D, Bailén G, Serrano M, Guillén F, Valverde JM, Zapata P, Castillo S, Valero D. (2007) Tools to maintain postharvest fruit and vegetable quality through the inhibition of ethylene action: a review. *Crit. Rev. Food Sci. Nutr*. **47**: 543-560.

Mata CI, Van de Poel B, Hertog ML, Tran D, Nicolai BM. (2018) Transcription analysis of the ethylene receptor and CTR genes in tomato: the effects of on and off-vine ripening and 1-MCP. *Postharvest Biol. Tech.* **140**: 67-75.

Menda N, Semel Y, Peled D, Eshed Y, Zamir D. (2004) In silico screening of a saturated mutation library of tomato. *Plant J.* **38**: 861-872.

Mohan V, Gupta S, Thomas S, Mickey H, Charakana C, Chauhan VS, Sharma K, Kumar R, Tyagi K, Sarma S, Gupta SK, Kilambi HV, Nongmaithem S, Kumari A, Gupta P, Sreelakshmi Y, Sharma R. (2016) Tomato fruits show wide phenomic diversity but fruit developmental genes show low genomic diversity. *PLoS One* **11:** e0152907.

Mubarok S, Hoshikawa K, Okabe Y, Yano R, Tri MD, Ariizumi T, Ezura H. (2019) Evidence of the functional role of the ethylene receptor genes SlETR4 and SlETR5 in ethylene signal transduction in tomato. *Mol. Genet. Genomics.* **294**: 301-313.

Muday GK, Rahman A, Binder BM. (2012) Auxin and ethylene: collaborators or competitors?. *Trends Plant Sci.* **17**: 181-195.

Nakatsuka A, Murachi S, Okunishi H, Shiomi S, Nakano R, Kubo Y, Inaba A. (1998) Differential expression and internal feedback regulation of 1-aminocyclopropane-1-carboxylate synthase, 1-aminocyclopropane-1-carboxylate oxidase, and ethylene receptor genes in tomato fruit during development and ripening. *Plant Physiol.* **118**: 1295-1305.

Negi S, Sukumar P, Liu X, Cohen JD, Muday GK. (2010) Genetic dissection of the role of ethylene in regulating auxin-dependent lateral and adventitious root formation in tomato. *Plant J.* **61**: 3-15.

Nogueira M, Mora L, Enfissi EM, Bramley PM, Fraser PD. (2013) Subchromoplast sequestration of carotenoids affects regulatory mechanisms in tomato lines expressing different carotenoid gene combinations. *Plant Cell* **25**: 4560-4579.

Oeller PW, Lu MW, Taylor LP, Pike DA, Theologis A. (1991). Reversible inhibition of tomato fruit senescence by antisense RNA. *Science*. **254**: 437-439.

Okabe Y, Asamizu E, Saito T, Matsukura C, Ariizumi T, Brès C, Rothan C, Mizoguchi T, Ezura H. (2011) Tomato TILLING technology: development of a reverse genetics tool for

the efficient isolation of mutants from Micro-Tom mutant libraries. *Plant Cell Physiol.* **52**: 1994-2005

Osorio S, Alba R, Damasceno CM, Lopez-Casado G, Lohse M, Zanor MI, Tohge T, Usadel B, Rose JK, Fei Z, Giovannoni JJ, Fernie AR. (2011) Systems biology of tomato fruit development: combined transcript, protein, and metabolite analysis of tomato transcription factor (nor, rin) and ethylene receptor (Nr) mutants reveals novel regulatory interactions. *Plant Physiol.* **157**: 405-425.

Pan X, Welti R, Wang X. (2010) Quantitative analysis of major plant hormones in crude plant extracts by high performance liquid chromatography-mass spectrometry. *Nature Protocols*. **5**: 986-992.

Pieterse CM, Leon-Reyes A, Van der Ent S, Van Wees SC. (2009) Networking by small-molecule hormones in plant immunity. *Nature Chem. Biol.* **5**: 308-316.

Pirrello J, Jaimes-Miranda F, Sanchez-Ballesta MT, Tournier B, Khalil-Ahmad Q, Regad F, Latche A, Pech JC, Bouzayen M. (2006) Sl-ERF2, a tomato ethylene response factor involved in ethylene response and seed germination *Plant Cell Physiol.* **47**: 1195-1205.

Qin G, Wang Y, Cao B, Wang W, Tian S. (2012) Unraveling the regulatory network of the MADS box transcription factor RIN in fruit ripening. *Plant J.* **70**: 243-255.

Roessner U, Wagner C, Kopka J, Trethewey RN, Willmitzer L. (2000) Simultaneous analysis of metabolites in potato tuber by gas chromatography-mass spectrometry. *Plant J.* **23**: 131-142.

Rottmann WH, Peter GF, Oeller PW, Keller JA, Shen NF, Nagy BP, Taylor LP, Campbell AD, Theologis A. (1991) 1-aminocyclopropane-1- carboxylate synthase in tomato is encoded by a multigene family whose transcription is induced during fruit and floral senescence. *J. Mol. Biol.* **222:** 937–961.

Santisree P, Nongmaithem S, Vasuki H, Sreelakshmi Y, Ivanchenko MG, Sharma R. (2011) Tomato Root Penetration in Soil Requires a Co-action between Ethylene and Auxin Signaling. *Plant Physiol.* **156:** 1424-1438

Seymour GB, Chapman NH, Chew BL, Rose JK. (2013) Regulation of ripening and opportunities for control in tomato and other fruits. *Plant Biotechnol. J.* **11:** 269-278.

Shu K, Liu XD, Xie Q, He ZH. (2016) Two faces of one seed: hormonal regulation of dormancy and germination. *Mol. Plant*. **9**: 34-45.

Sim NL, Kumar P, Hu J, Henikoff S, Schneider G, Ng PC. (2012) SIFT web server: predicting effects of amino acid substitutions on proteins. *Nucleic Acids Res.* **40(W1)**: W452-457.

Sisler EC, Dupille E, Serek M. (1996) Effect of 1-methylcyclopropene and methylenecyclopropane on ethylene binding and ethylene action on cut carnations. In *Plant Hormone Signal Perception and Transduction.* Eds Smith AR, Berry AW, Harpham NVJ, Moshkov IE, Novikova GV, Kulaeva ON, Hall MA. pp. 127-134 Springer, Dordrecht.

Sisler EC. (2006) The discovery and development of compounds counteracting ethylene at the receptor level. *Biotechnol. Adv.* **24**: 357-367.

Sreelakshmi Y, Gupta S, Bodanapu R, Chauhan VS, Hanjabam M, Thomas S, Mohan V, Sharma S, Srinivasan R, Sharma R. (2010) NEATTILL: A simplified procedure for nucleic acid extraction from arrayed tissue for TILLING and other high-throughput reverse genetic applications. *Plant Methods* **6:** 3

Su L, Diretto G, Purgatto E, Danoun S, Zouine M, Li Z, Roustan JP, Bouzayen M, Giuliano G, Chervin C. (2015) Carotenoid accumulation during tomato fruit ripening is modulated by the auxin-ethylene balance. *BMC Plant Biol.* **15**: 114.

Tanaka Y, Sano T, Tamaoki M, Nakajima N, Kondo N, Hasezawa S. (2005) Ethylene inhibits abscisic acid-induced stomatal closure in Arabidopsis. *Plant Physiol.***138**: 2337-2343.

Tanaka Y, Sano T, Tamaoki M, Nakajima N, Kondo N, Hasezawa S. (2006) Cytokinin and auxin inhibit abscisic acid-induced stomatal closure by enhancing ethylene production in Arabidopsis. *J. Exp. Bot.* **57**: 2259-2266.

Tarun AS, Lee JS, Theologis A. (1998) Random mutagenesis of 1-aminocyclopropane-1-carboxylate synthase: a key enzyme in ethylene biosynthesis. *Proc. Natl. Acad. Sci. USA* **95**: 9796-9801

Tatsuki M, Mori H. (2001) Phosphorylation of tomato 1-aminocyclopropane-1-carboxylic acid synthase, LE-ACS2, at the C-terminal region. *J. Biol. Chem*. **276**: 28051-28057.

Theologis A, Oeller PW, Wong LM, Rottmann WH, Gantz DM. (1993) Use of a tomato mutant constructed with reverse genetics to study fruit ripening, a complex developmental process. *Dev. Genet.* **14**: 282-295.

Tieman DM, Taylor MG, Ciardi JA, Klee HJ. (2000) The tomato ethylene receptors NR and LeETR4 are negative regulators of ethylene response and exhibit functional compensation within a multigene family. *Proc. Natl. Acad. Sci. USA*. **97**: 5663-5668.

Tígchelaar EC, Mcglasson WB, Franklin MJ. (1978) Natural and ethephon-stimulated ripening of F1 hybrids of the ripening inhibitor (rin) and non-ripening (nor) mutants of tomato (Lycopersicon esculentum Mill.). *Aust. J. Plant Physiol.* **5***:*449-456.

Till BJ, Zerr T, Comai L, Henikoff S. (2006) A protocol for TILLING and Ecotilling in plants and animals. *Nature Protocols*. **1**: 2465-2477.

Towbin H, Staehelin T, Gordon J. (1979) Electrophoretic transfer of proteins from polyacrylamide gels to nitrocellulose sheets: procedure and some applications. *Proc. Natl. Acad. Sci. USA*.**76**: 4350-4354.

Tsuchisaka A, Theologis A. (2004) Heterodimeric interactions among the 1-amino-cyclopropane-1-carboxylate synthase polypeptides encoded by the Arabidopsis gene family. *Proc. Natl. Acad. Sci. USA*. **101**: 2275-2280.

Tsuchisaka A, Yu G, Jin H, Alonso JM, Ecker JR, Zhang X, Gao S, Theologis A. (2009) A combinatorial interplay among the 1-aminocyclopropane-1-carboxylate isoforms regulates ethylene biosynthesis in Arabidopsis thaliana. *Genetics*. **183**: 979-1003.

Van de Poel B, Bulens I, Hertog ML, Nicolai BM, Geeraerd AH. (2014) A transcriptomics-based kinetic model for ethylene biosynthesis in tomato (Solanum lycopersicum) fruit: development, validation and exploration of novel regulatory mechanisms. *New Phytol.* **202**: 952-963.

Van de Poel B, Bulens I, Markoula A, Hertog ML, Dreesen R, Wirtz M, Vandoninck S, Oppermann Y, Keulemans J, Hell R, Waelkens E. (2012) Targeted systems biology profiling of tomato fruit reveals coordination of the Yang cycle and a distinct regulation of ethylene biosynthesis during postclimacteric ripening. *Plant Physiol.* **160**: 1498-1514.

Vrebalov J, Pan IL, Arroyo AJ, McQuinn R, Chung M, Poole M, Rose J, Seymour G, Grandillo S, Giovannoni J, Irish VF. (2009) Fleshy fruit expansion and ripening are regulated by the tomato SHATTERPROOF gene TAGL1. *Plant Cell*. **21**: 3041-3062.

Vrebalov J, Ruezinsky D, Padmanabhan V, White R, Medrano D, Drake R, Schuch W, Giovannoni J. (2002) A MADS-box gene necessary for fruit ripening at the tomato ripening-inhibitor (rin) locus. *Science*. **296**: 343-346.

Wilkinson JQ, Lanahan MB, Yen HC, Giovannoni JJ, Klee HJ. (1995) An ethylene-inducible component of signal transduction encoded by Never-ripe. *Science*. **270**: 1807-1809

Xia J, Mandal R, Sinelnikov IV, Broadhurst D, Wishart DS. (2012) MetaboAnalyst 2.0—a comprehensive server for metabolomic data analysis. *Nucleic Acids Res.* **40(W1**): W127-133.

Yan R, Yokotani N, Yamaoka T, Ushijima K, Nakano R, Yano K, Aoki K, Kubo Y. (2013). Characterization of ripening-associated genes using a tomato DNA macroarray, 1-methylcyclopropene, and ripening-impaired mutants. *Postharvest. Biol. Tec.* **86**:159-157

Yang SF, Hoffman NE. (1984) Ethylene biosynthesis and its regulation in higher plants. *Annu. Rev. Plant Physiol. 3*5:155–189

Yang Y-X, Ahammed G, Wu C, Fan S, Zhou Y-H. (2015). Crosstalk among Jasmonate, Salicylate and Ethylene Signaling Pathways in Plant Disease and Immune Responses. *Curr. Protein Pept. Sc.* **16:** 450–461.

Yokotani N, Nakano R, Imanishi S, Nagata M, Inaba A, Kubo Y. (2009). Ripening-associated ethylene biosynthesis in tomato fruit is autocatalytically and developmentally regulated. *J. Exp. Bot.* **60**: 3433–3442.

Zhang M, Yuan B, Leng P. (2009) The role of ABA in triggering ethylene biosynthesis and ripening of tomato fruit. *J. Exp. Bot.* **60**: 1579-1588.

Zheng S, Kim H, Verhaak RGW. (2014) Silent mutations make some noise. *Cell* **156:** 1129–1131

Zhong S, Fei Z, Chen YR, Zheng Y, Huang M, Vrebalov J, McQuinn R, Gapper N, Liu B, Xiang J, Shao Y, Giovannoni JJ. (2013) Single-base resolution methylomes of tomato fruit development reveal epigenome modifications associated with ripening. *Nature Biotechnol.* **31**: 154-159.

Figure 1

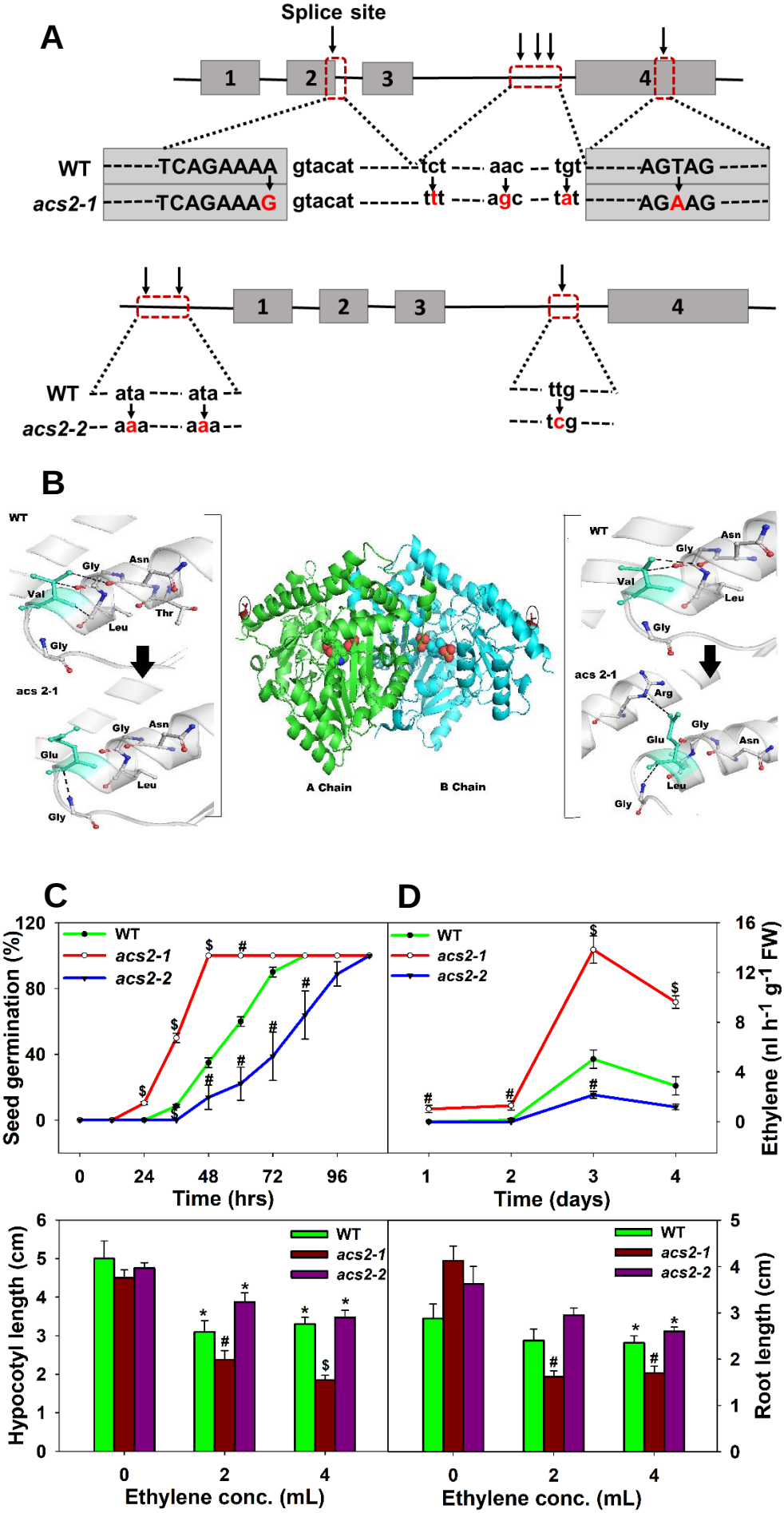

Figure 2

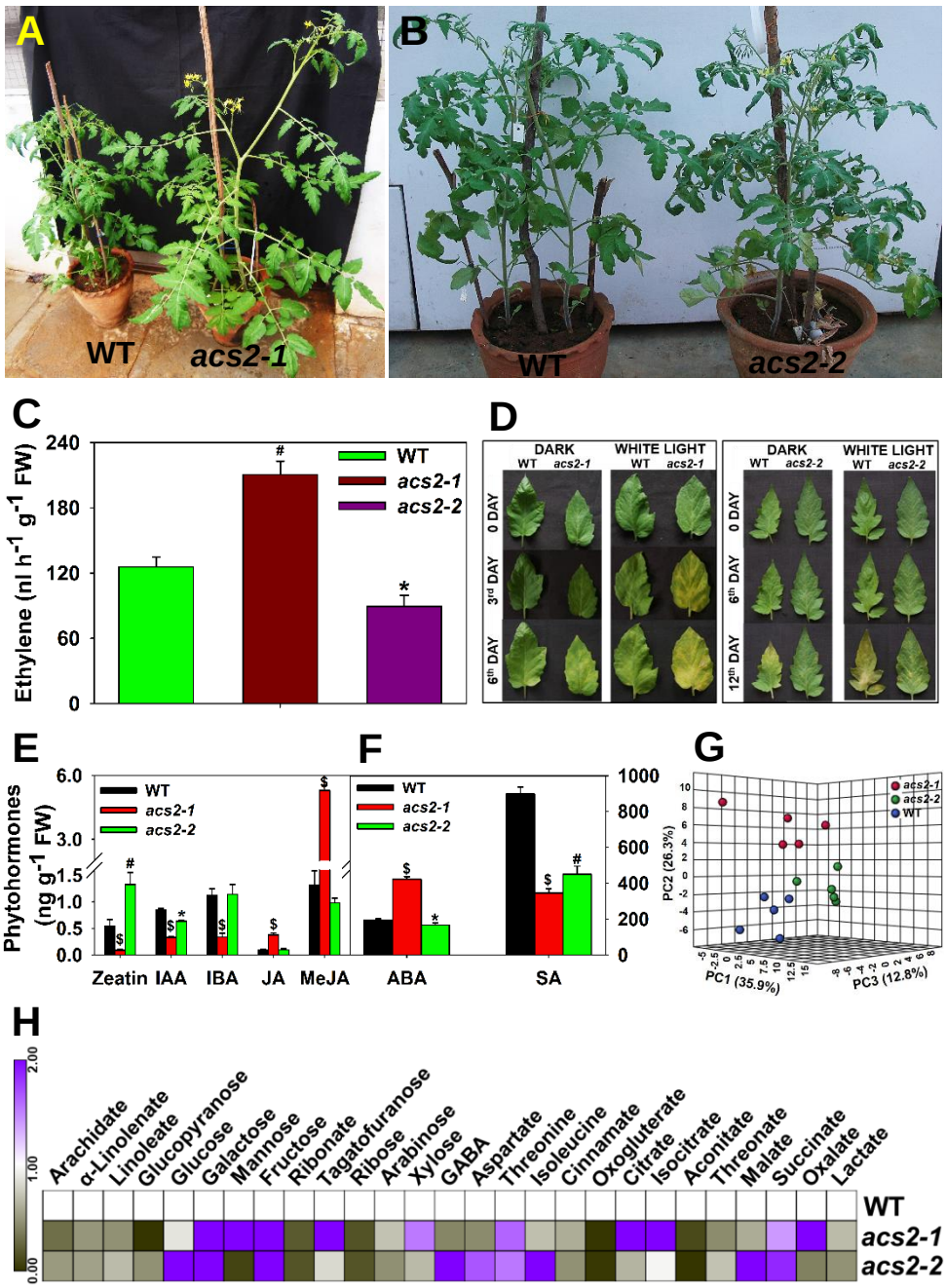

Figure 3

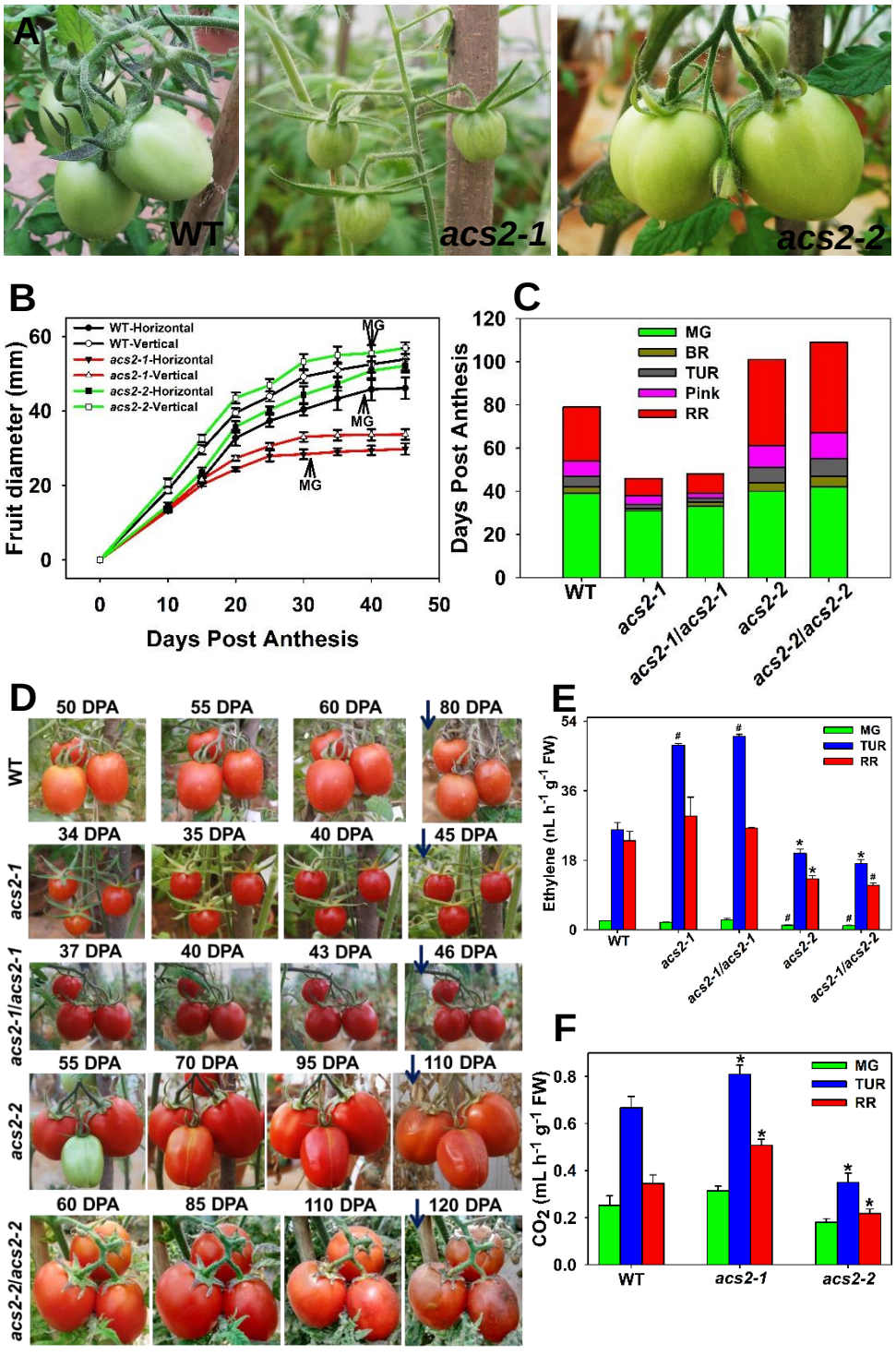

Figure 4

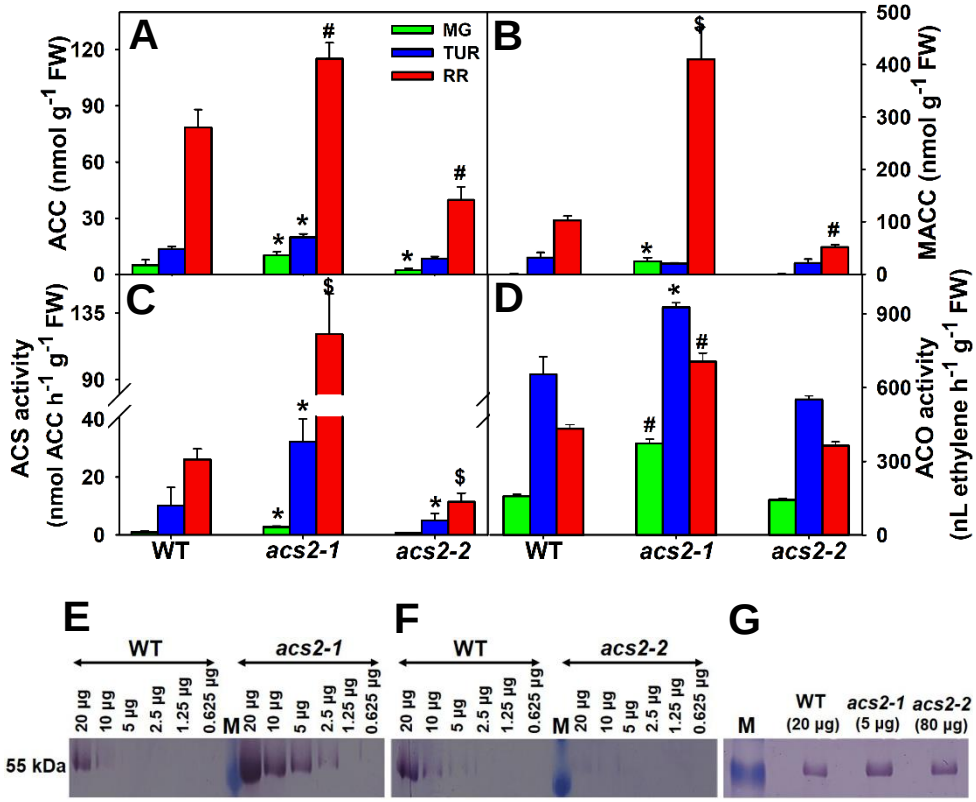

Figure 5

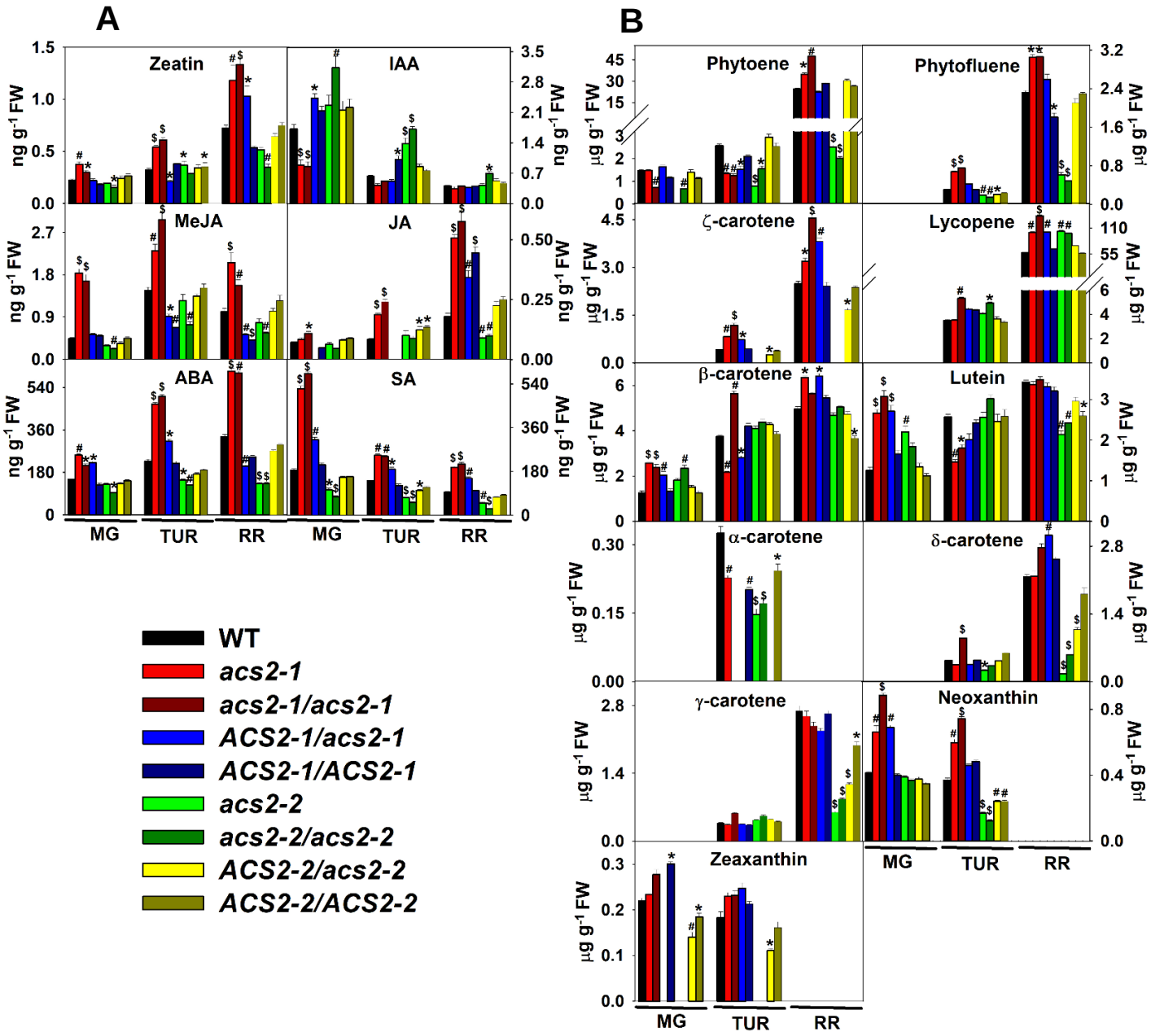

Figure 6

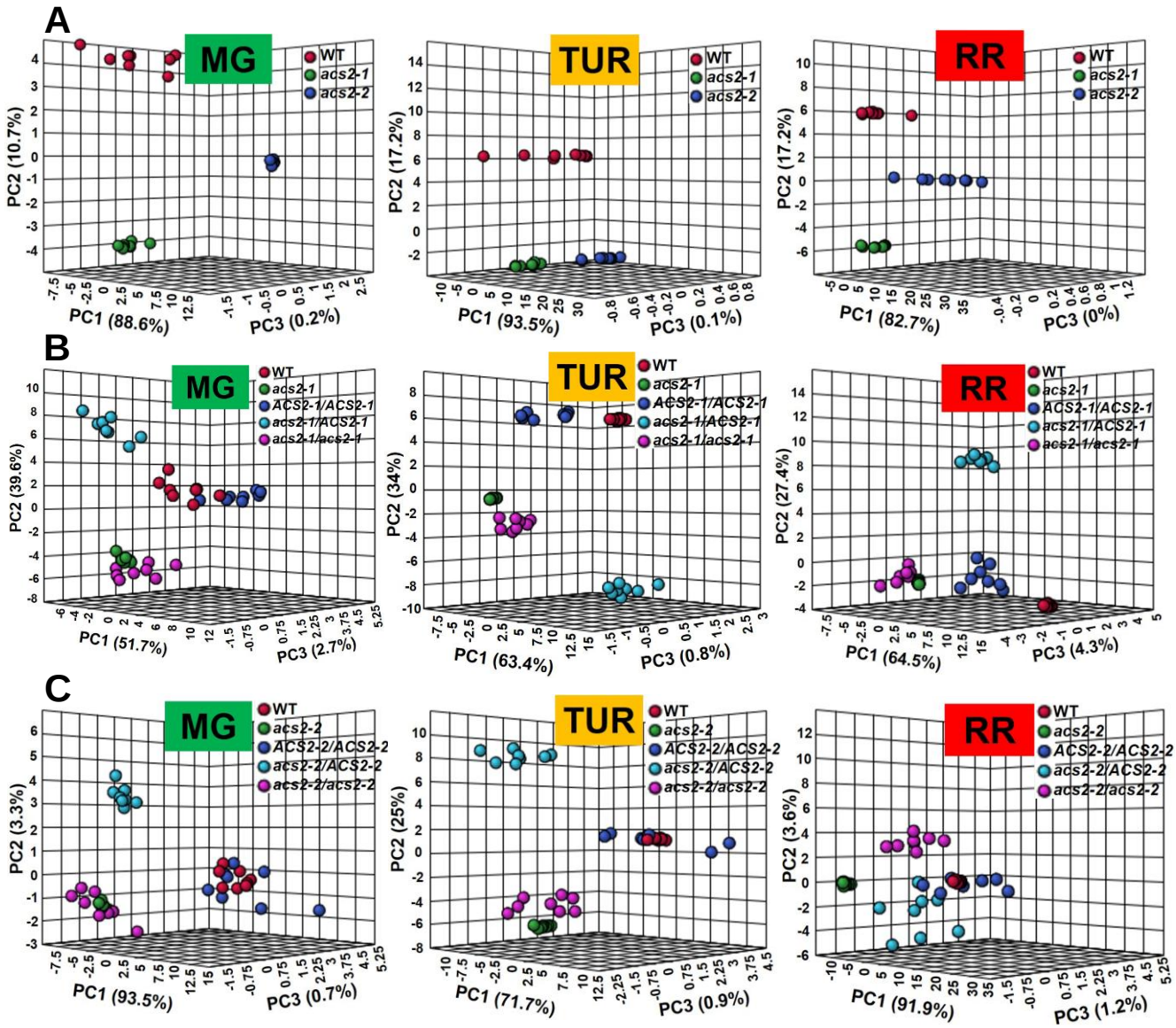

Figure 7

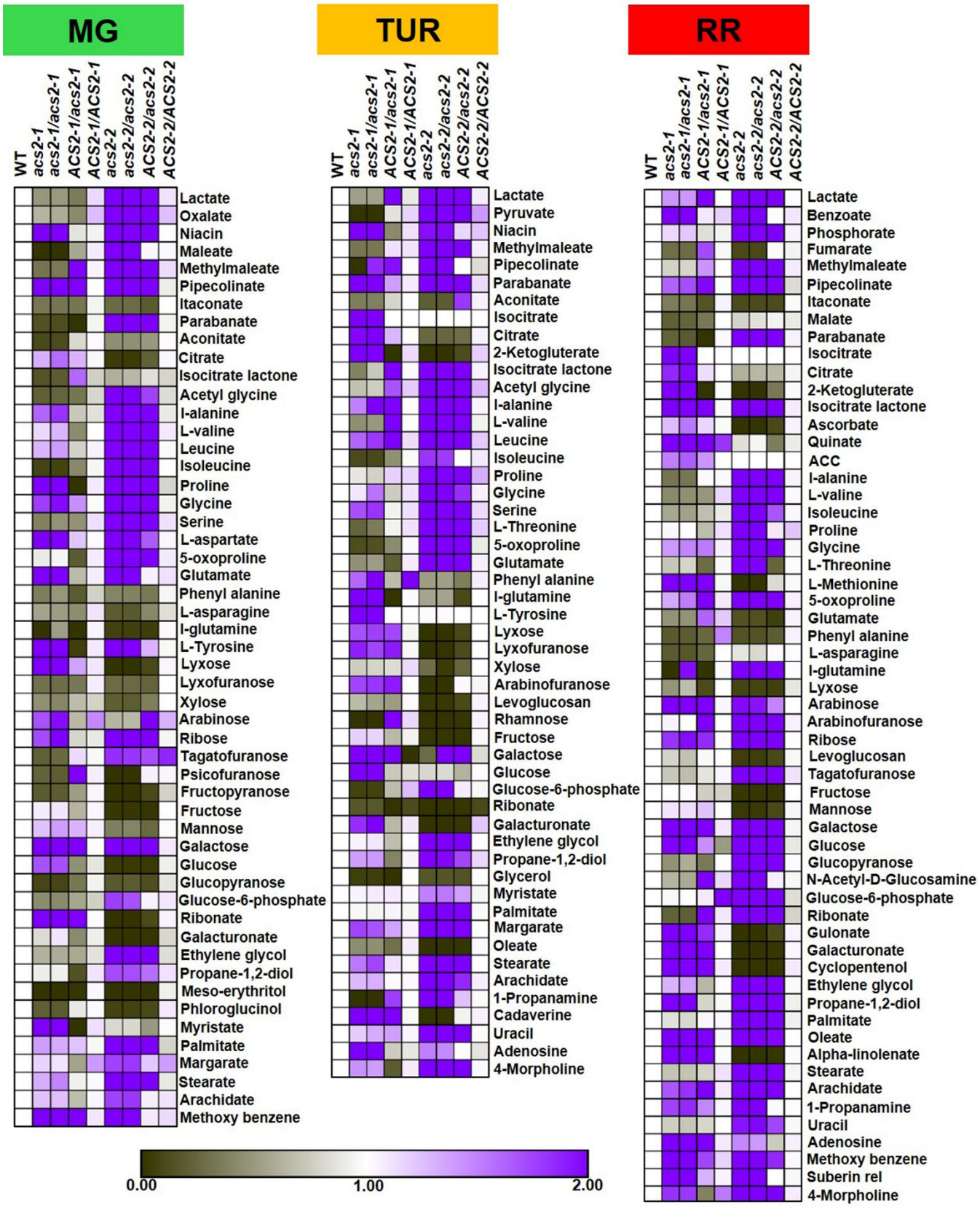

Figure 8

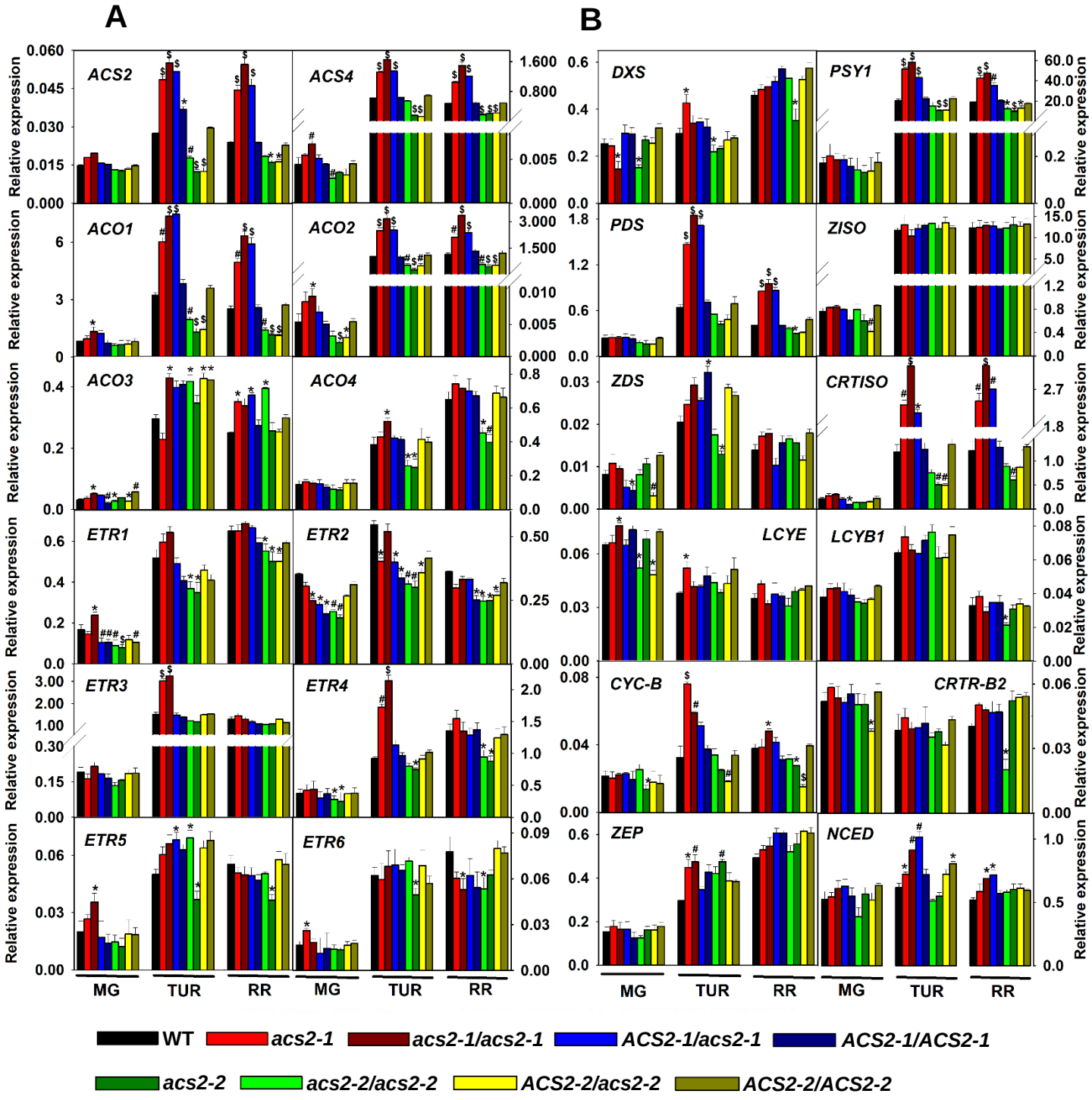

Figure 9

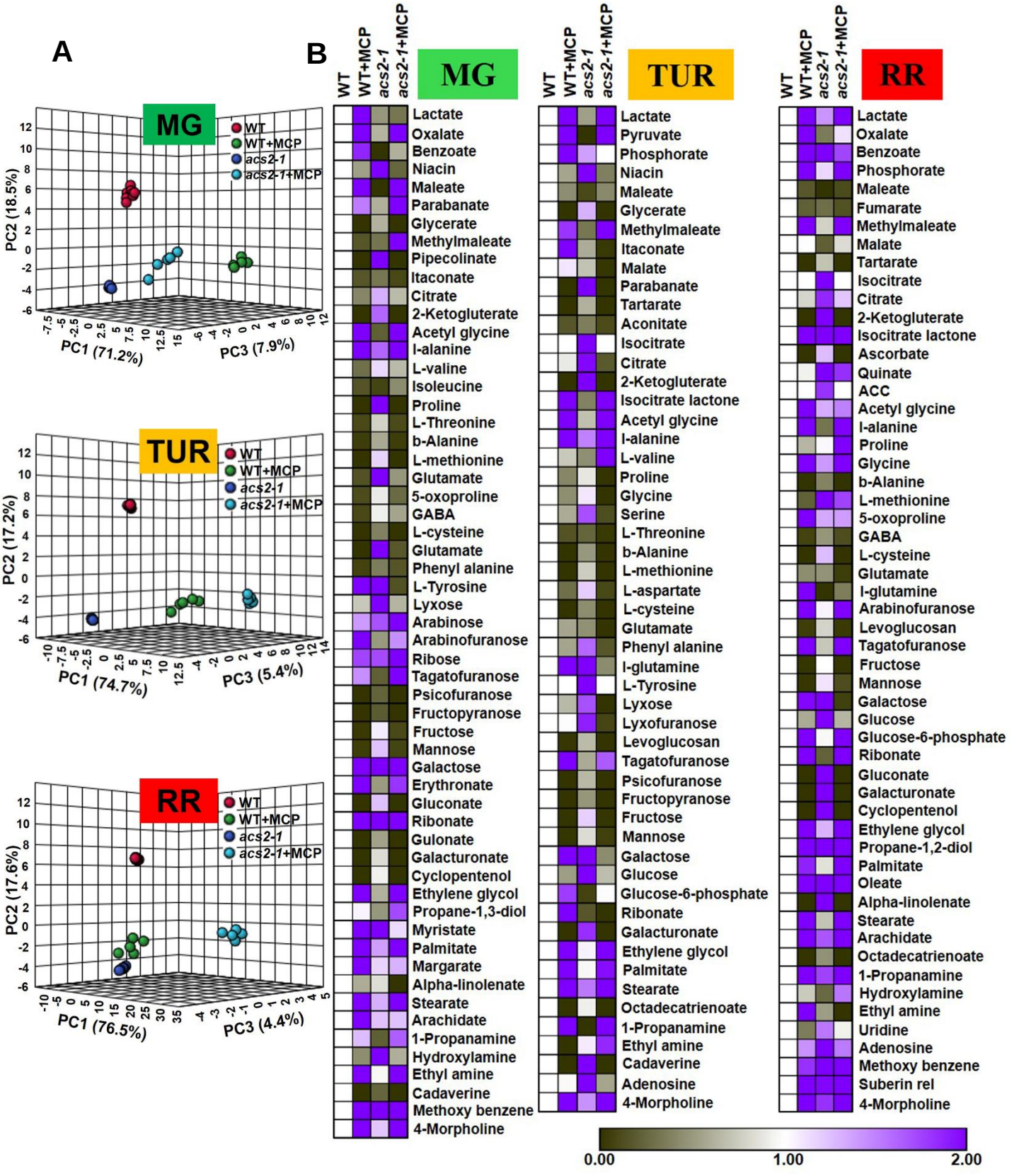

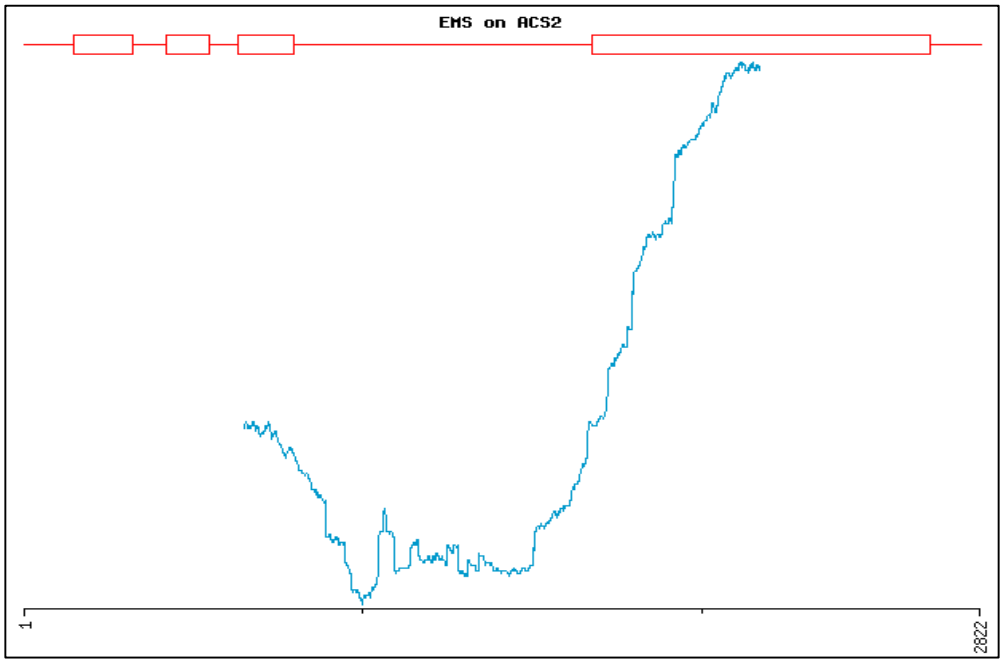

Supplemental Figure 1. Prediction of region susceptible to deleterious mutation in the *ACS2* (Solyc01g095080.2.1) gene by CODDLE software (http://blocks.fhcrc.org/proweb/coddle, last accessed in August 2017). The red boxes correspond to exons, whereas the line joining two boxes represents the introns.

A

Donor splice sites, direct strand

pos 5'->3'	phase	strand	confidence	5' exon intron 3'
399	0	+	0.74	ATTCAGAAAA^GTACATATCG

B

Donor splice sites, direct strand

pos 5'->3'	phase	strand	confidence	5' exon intron 3'
399	0	+	1.00	ATTCAGAAAG^GTACATATCG H

Supplemental Figure 2. Splice site analysis of *acs2-1* mutant by NetGene2 server. **A** represents the WT splice site, while **B** represents the mutant splice site. Red circle denotes the site of changed base in mutant. The increase in confidence denotes more efficient splicing of transcript.

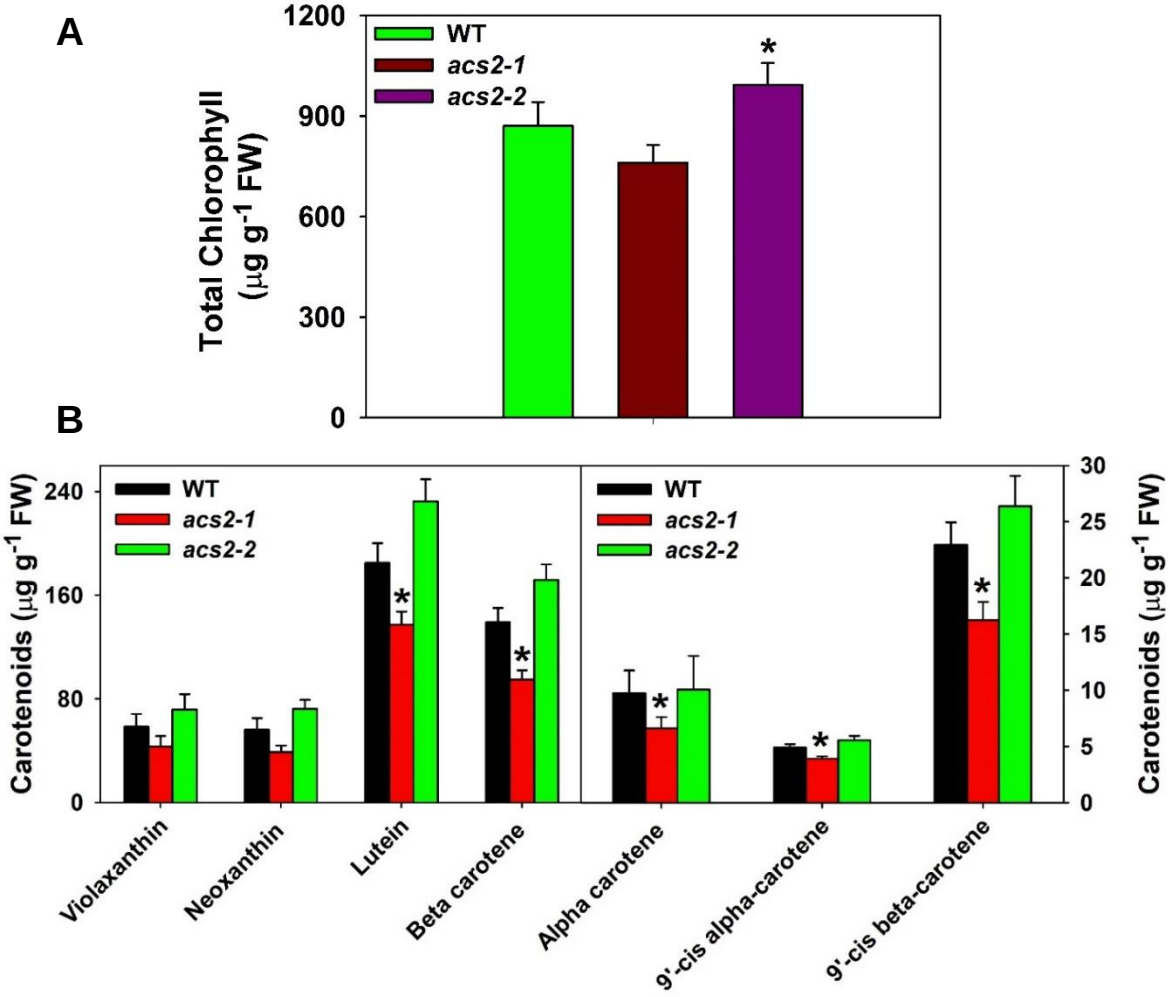

Supplemental Figure 3. Chlorophyll (**A**), carotenoids, and xanthophylls (**B**) levels in the leaf of WT, *acs2-1*, and *acs2-2* mutant. Leaves were harvested from the seventh node of 45-day-old plants of wild type and mutants. (Student's t-test; * for $P \leq 0.05$, # for $P \leq 0.01$ and $ for $P \leq 0.001$, for chlorophyll and carotenoid estimation, sample number, n= 5 ± SE).

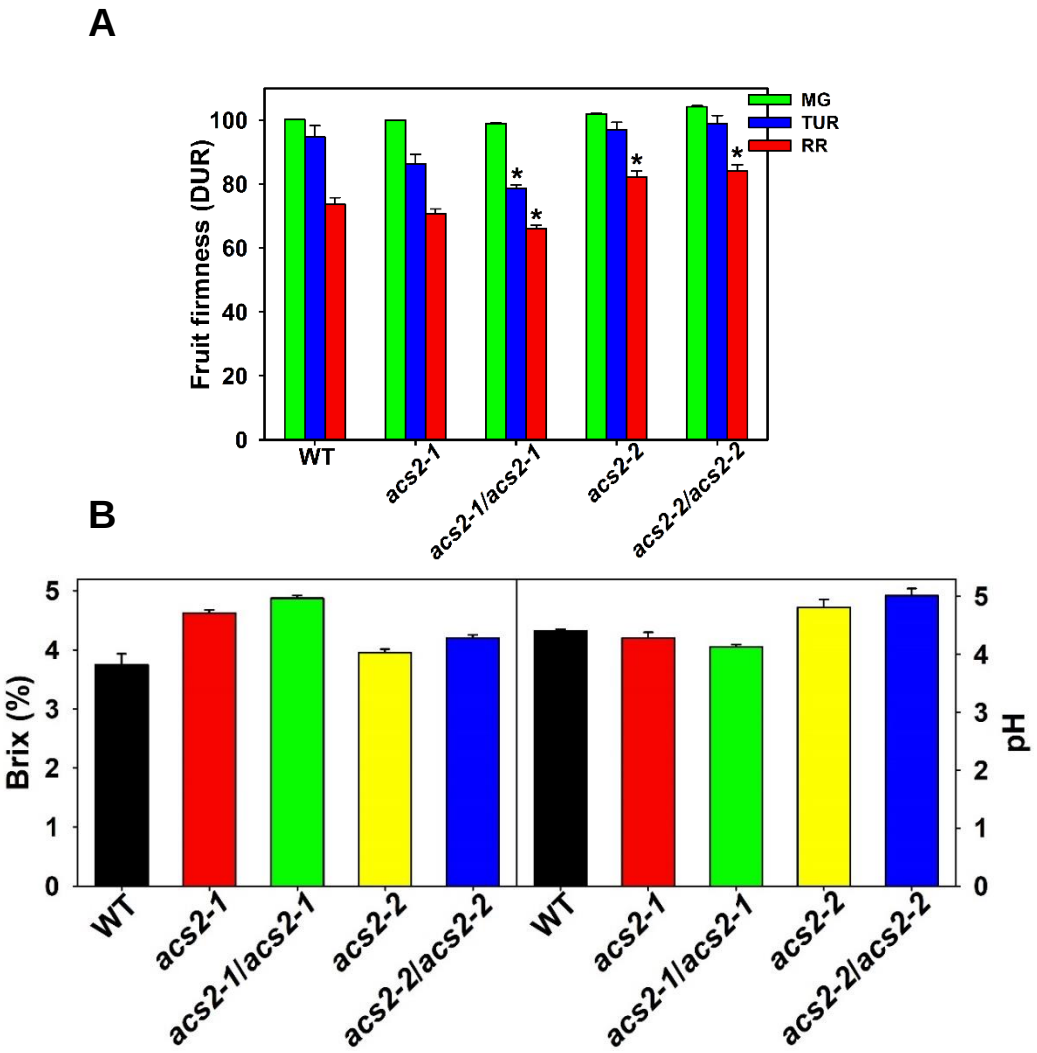

Supplemental Figure 4. Fruit firmness (**A**), total soluble solids (Brix) (**B**), and pH (**C**) of WT, *acs2* mutants, and their BC_1F_2 progenies at different ripening stages. Firmness value was recorded by measuring each fruit at equatorial plane two-three times. (Student's t-test; * for $P \leq 0.05$, # for $P \leq 0.01$ and $ for $P \leq 0.001$, n=3 ± SE).

A.

>sp|P18485|1A12_SOLLC 1-aminocyclopropane-1-carboxylate synthase 2 OS=Solanum lycopersicum GN=ACS2 PE=1 SV=2

MGFEIAKTNSILSKLATNE**EHGENSPYFDGWKAYDSD**PFHPLKNPNGVIQM
GLAENQLCLDLIEDWIKRNPKGSICSEGIKSFKAIANFQDYHGLPEFRKAIA
KFMEKTRGGRVRFDPERVVMAGGATGANETIIFCLADPGDAFLVPSPYYPA
FNRDLRWRTGVQLIPIHCESSNNFKITSKAVKEAYENAQKSNIKVKGLILTN
PSNPLGTTLDKDTLKSVLSFTNQHNIHLVCDEIYAATVFDTPQFVSIAEILDE
QEMTYCNKDLVHIVYSLSKDMGLPGFRVGIIYSFNDDVVNCARKMSSFGLV
STQTQYFLAAMLSDEKFVDNFLRESAMRLGKRHKHFTNGLEVVGIKCLKN
NAGLFCWMDLRPLLRESTFDSEMSLWRVIINDVKLNVSPGSSFECQEPGWF
RVCFANMDDGTVDIALARIRRFVGVEKSG**DKSSSMEKKQQWKKNNLR**LSF
SKRMYDESVLSPLSSPIPPSPLVR

B.

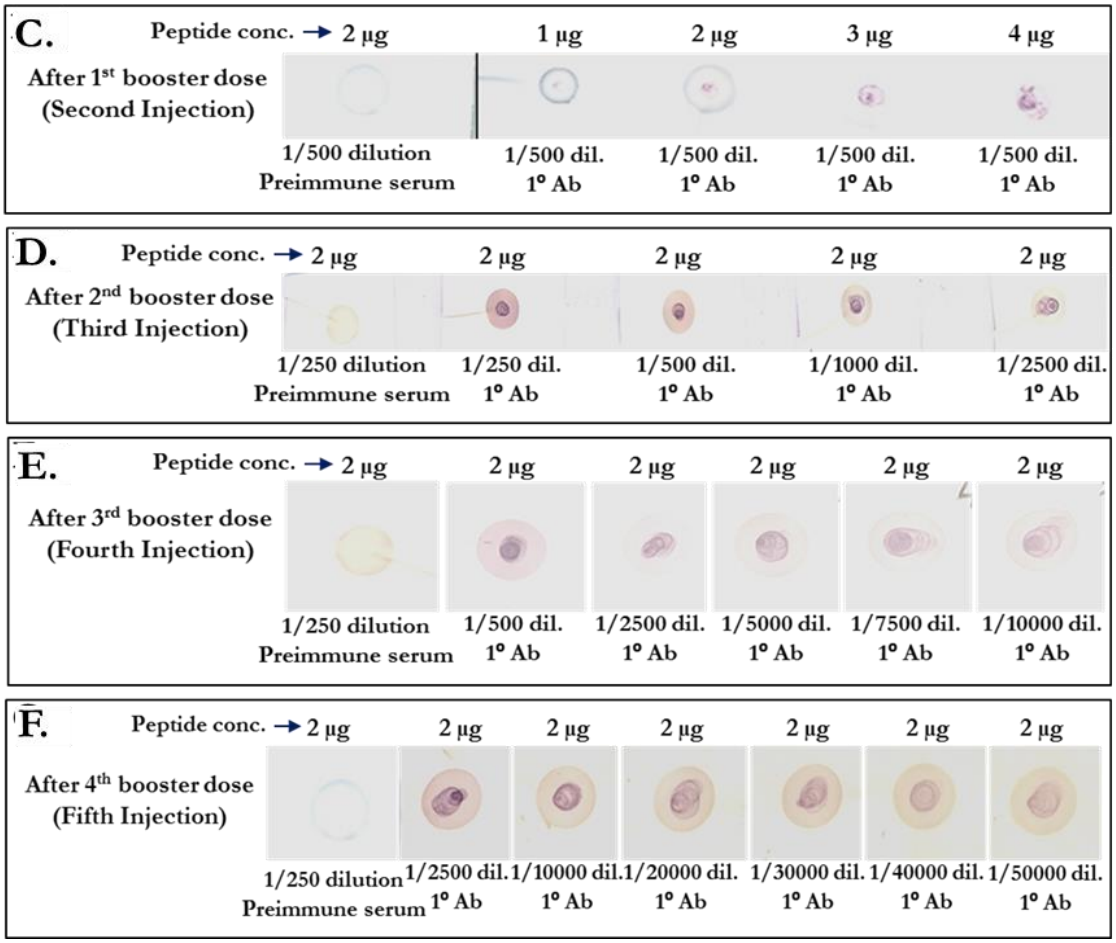

Supplemental Figure 5. Raising and validation of antibodies specific for ACS2 peptides. Three antigenic peptides (marked in red) specific to ACS2 protein were predicted by PEPTIDE 2.0 (https://www.peptide2.com). Out of three peptides, N-terminal region peptide "EHGENSPYFDGWKAYDSD" specific to ACS2 protein was selected for antibody raising and was synthesized by PEPTIDE 2.0 **(A)**. The small aliquots of antisera from rabbit were collected after 1st, 2nd, 3rd, and 4th booster dose and checked for antibody titer value by DOT BLOT assay **(B-E)**.

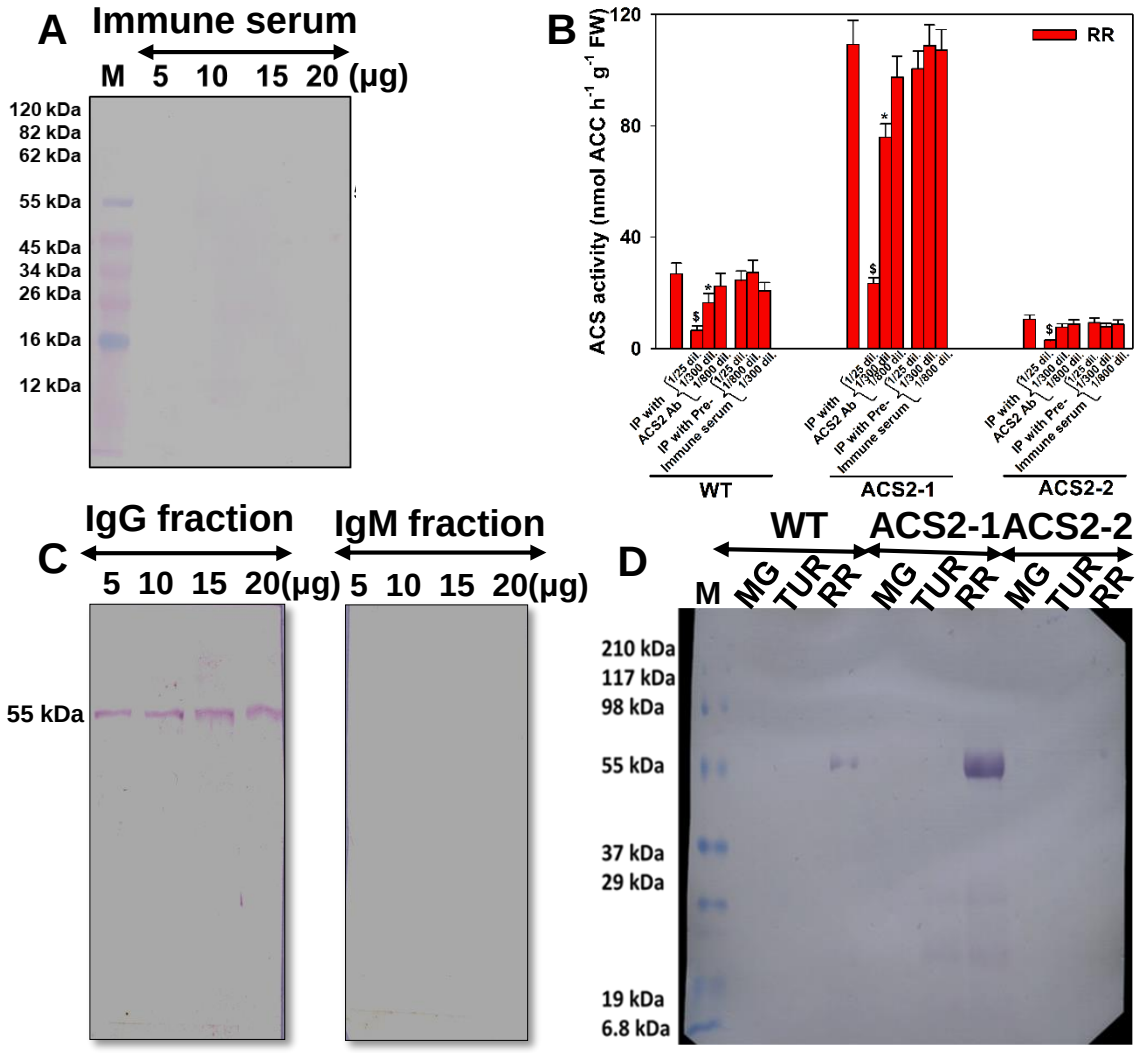

Supplemental Figure 6. Immunoprecipitation and Western blotting of ACS2 protein using purified IgG fraction. **(A)** Varying amount (5-20 µg) of crude extract of wild-type red-ripe fruits was resolved on SDS-PAGE gel with protein marker (**M**), and Western blotting was performed using unpurified immune serum. **(B)** Immunoprecipitation of ACS protein was carried out in crude extract of wild-type red-ripe fruits with protein-A Sepharose beads. After precipitating antigen-antibody complex, the supernatants were analyzed for the ACS activity. (Student's t-test; * for $P \leq 0.05$, # for $P \leq 0.01$ and $ for $P \leq 0.001$, for each fruit maturity stage, n=3 ± SE). **(C)** The immunoprecipitated ACS2 protein was resolved on the SDS-PAGE gel. The Western blotting was performed using purified IgG (Left) and IgM fraction (Right) of antiserum. **(D)** Western blot assay of immunoprecipitated ACS2 protein at different stages of tomato fruit ripening. IgG-mediated, immunoprecipitated ACS2 protein content was quantified by Bradford's assay. An equal amount (20 µg) of immunoprecipitated protein from different ripening stages of tomato fruits of WT and mutants was resolved on SDS-PAGE gel.

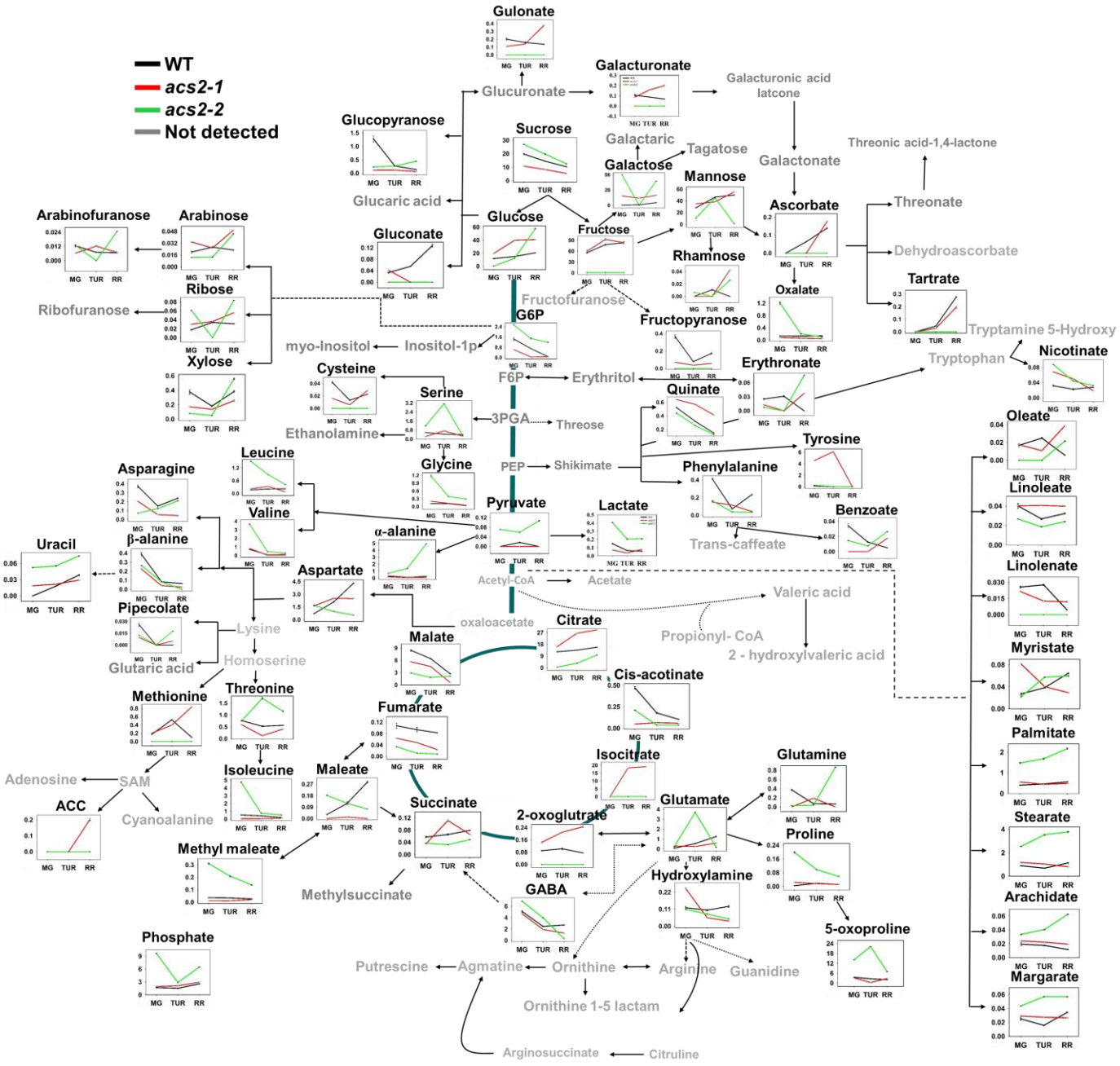

Supplemental Figure 7. The metabolic shifts in *acs2* mutant fruits during ripening in comparison to WT. An overview of the metabolic pathways representing relative abundance of metabolites at different ripening stages in fruits of WT, *acs2-1*, and *acs2-2* mutants. The Y-axis represents the relative levels of metabolites with reference to internal standard ribitol. X axis denotes metabolite levels at MG- mature green, TUR- turning, and RR- red-ripe stages.

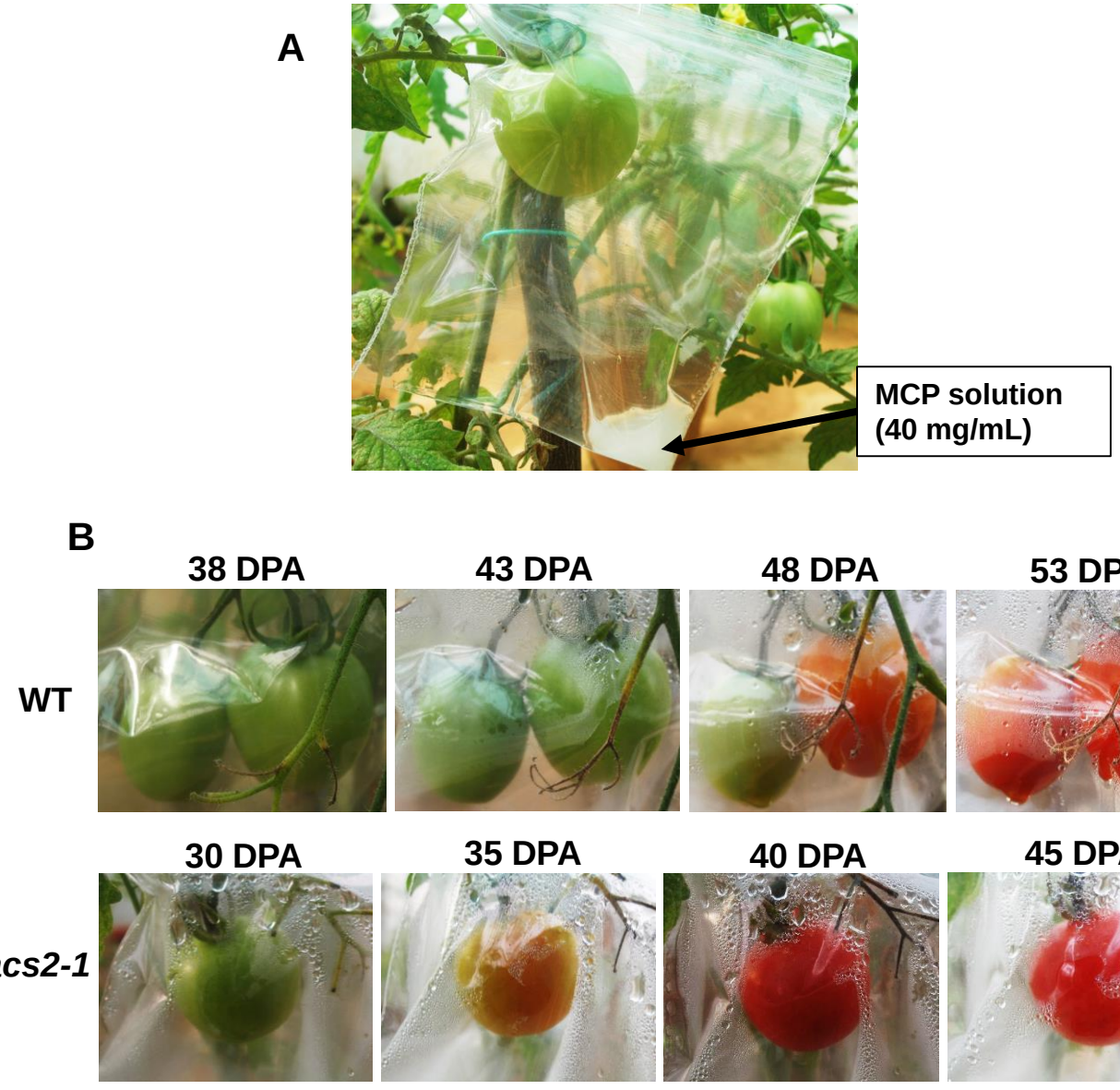

Supplemental Figure 8. On-vine treatment of MCP to mature green fruits of WT and *acs2-1* mutant. **(A)** Depicts experimental setup for the on-vine treatment of MCP to MG fruits. **(B)** Fruits were visually monitored for change in color after treatment with MCP. Representative photograph shows delayed ripening in WT and *acs2-1* mutant. Five biological replicates were considered for the experiment.

Supplemental Table 1. EMS-mutagenized tomato populations used for the isolation of *ACS2* mutants. Four different EMS-mutagenized populations were screened for detection of mutations in *ACS2* gene (Solyc01g095080.2.1) using TILLING. The number of mutagenized plants screened is indicated in the table.

Population Number	Tomato cultivar	EMS concentration	Generation used for DNA pooling	Population size	Number of *acs-2* mutant alleles identified
I	Arka Vikas	60 mM	M_2	3768	5
II	Arka Vikas	120 mM	M_2	768	1
III	M82	60 mM	M_2*	1536	2
IV	M82	60 mM	M_3	3072	1

*The population III was obtained from Dani Zamir, Hebrew University, Israel. The raising of this population is described in Menda et al., (2014). The population IV consisted of M_3 seeds harvested from population III.

Reference:

Menda N, Semel Y, Peled D, Eshed Y, Zamir D. (2004) In silico screening of a saturated mutation library of tomato. *The Plant Journal.* **38**: 861- 872.

Supplemental Table 2. *ACS2* Mutant lines identified and confirmed for mutation. The position of mutation was confirmed by Multialin Interface page (Corpet et al., 1988) using WT DNA as a template sequence. The changes in amino acids were obtained after the translation of mutated ORF sequence, The effect of the non-synonymous mutation on protein function was determined by using SIFT software version 4.0.5 (https://sift.bii.a-star.edu.sg/). The PSSM difference was obtained using NCBI PSSM viewer (https://www.ncbi.nlm.nih.gov/Class/Structure/pssm/pssm_viewer.cgi)

Mutants identified	Position of mutation	Change in Amino acid	PSSM Difference	SIFT Score	Promoter element modified
acs2-1 (Solyc01g095080.2.1) (M82-M3-112)	A398G	K100=	Nil	1.0	-
	C1343T	Intron3	-	-	-
	A1383G	Intron3	-	-	-
	G1410A	Intron3	-	-	-
	T2119A	V352E	- 9.7	0.735	-
acs2-2 (Solyc01g095080.2.1) (M82-M3-162A)	T-382A	Promoter	-	-	AAAA**T**ATTT **WT** AAAA**A**ATTT ***acs2-2***
	T-106A	Promoter	-	-	ACAA**T**AAAA **WT** ACAA**A**AAAA ***acs2-2***
	T1409C	Intron3	-	-	

Reference:

Corpet F, Gouzy J, Kahn D. (1998) The ProDom database of protein domain families. *Nucleic Acids Research.* **26**: 323- 326.

Supplemental Table 3. The genetic segregation of *acs2-1* and *acs2-2* mutants in BC_1F_2 generation. The presence of mutated gene copy and its zygosity in backcrossed plants was monitored by the CEL- I endonuclease assay (Mohan et al., 2016). In brief, we used PCR based mutation screening which involves three steps – firstly, amplification of a fragment of interest followed by heteroduplex formation and mismatch cleavage by CEL-I enzyme and finally, detection on denaturing polyacrylamide gels.

Crosses	**BC_1F_2 Population size**	**BC_1F_2 (WT homozygous) (+/+)**	**BC_1F_2 (heterozygous) (+/-)**	**BC_1F_2 (mutant homozygous) (- /-)**	**χ^2**	**P-Value**
acs2-1♂ **X** WT♀	120	30	61	29	0.224 (**3:1**) 0.245 (**1:2:1**)	0.62 (**3:1**) 0.88 (**1:2:1**)
acs2-2♂ **X** WT♀	108	27	56	25	0.101 (3:1) 0.113 (**1:2:1**)	0.95 (3:1) 0.94 (**1:2:1**)

Reference:

Mohan V, Gupta S, Thomas S, Mickey H, Charakana C, Chauhan VS, Sharma K, Kumar R, Tyagi K, Sarma S, Gupta SK, Kilambi HV, Nongmaithem S, Kumari A, Gupta P, Sreelakshmi Y, Sharma R (2016) Tomato fruits show wide phenomic diversity but fruit developmental genes show low genomic diversity. *PLoS One* **11:** e0152907.

Supplemental Table 4. Increase in ACS2-1 protein stability predicted by different software. The impact of the mutations in *acs2-1* on the stability of ACS2-1 protein was analyzed using five different software (CUPSAT, MAESTROWeb, PoPMuSiCv3.1, STRUM, and DynaMut). All software predicted that the mutated protein to be more stable than the wild type.

Tool	Chain A ΔΔG (kcal/mol)	Chain B ΔΔG (kcal/mol)	Stabilizing/ Unstabilizing	Link
CUPSAT	0.77	0.91	Stabilizing	http://cupsat.tu- bs.de/
MAESTROWeb	- 0.406	- 0.406	Stabilizing	https://pbwww.che.sbg.ac.at/maestro/web
PoPMuSiCv3.1	- 0.34	- 0.34	Stabilizing	https://soft.dezyme.com/query/create/pop
STRUM	- 0.34	- 0.34	Stabilizing	https://zhanglab.ccmb.med.umich.edu/STRUM/
DynaMut	0.38	0.223	Stabilizing	http://biosig.unimelb.edu.au/dynamut/

ΔΔG: The change in Gibbs free energy. The above software predicted that observed changes **ΔΔG** due to point mutation stabilizes the mutated protein.

Supplemental Table 5. **The alteration of bonding pattern in ACS2 protein in *acs2-1* mutant compared to WT protein.** The interacting amino acids are denoted by respective alphabets (capital). The bonding atoms in each amino acid are represented in parentheses, and bond length is denoted in angstroms (Å). The novel amino acid interactions appearing in mutant proteins are highlighted in Figure 1B of the main manuscript. The values presented in the table were obtained using Dynamut software (http://biosig.unimelb.edu.au/dynamut/)

WT A chain		***acs2-1* A chain**			**WT B chain**		***acs2-1* B chain**		
Amino acid bonding	**Bond length and type of bond**	**Amino acid bonding**	**Bond length and type of bond**	**Remarks**	**Amino acid bonding**	**Bond length and type of bond**	**Amino acid bonding**	**Bond length and type of bond**	**Remarks**
V352(N)→ N348(O)	3.2 Å H bond - VDW	E352(N)→ N348(O)	3.2 Å H bond- proximal	VDW changes to proximal	V352(N)→ N348(O)	3 Å H Bond- VDW clash	E352(N)→ N348(O)	3 Å H bond- VDW clash	No change
V352(C)→ N348(O)	2.9 Å weak H bond- VDW clash			**Not present in mutant**	V352(C)→ N348(O)	3.3 Å Weak H bond- VDW			**Not present in mutant**
V352(N)→ G349(O)	3 Å H bond - VDW clash	E352(N)→. G349(O)	3.1 Å H bond - VDW clash	Increase in bond length **Not present in B chain**					
V352(C)→ G349(O)	3.1 Å weak H bond - VDW clash	E352(C)→ G349(O)	3.4 Å weak Polar Proximal	Increase in bond length **Not present in B chain**	V352(C)→ G349(O)	3.5 Å Weak H bond- Proximal			**Not present in mutant**
V352(N)→ L350(C)	3.3 Å Undefined- VDW			**Not present in mutant A chain**	V352(N)→ L350(C)	3 Å Undefined- VDW clash	E352(N)→ L350(C)	3.1 Å Undefined- VDW clash	Increase in bond length
					V352(N)→ L350(O)	3.2 Å Polar- proximal	E352(N)→ L350(O)	3.3 Å Polar- Proximal	Increase in bond length, **Not present in A chain**

WT A chain		***acs2-1* A chain**			**WT B chain**		***acs2-1* B chain**		
Amino acid bonding	**Bond length and type of bond**	**Amino acid bonding**	**Bond length and type of bond**	**Remarks**	**Amino acid bonding**	**Bond length and type of bond**	**Amino acid bonding**	**Bond length and type of bond**	**Remarks**
					V352(C)→ G354(N)	3.1 Å Undefined- VDW clash	E352(C)→ G354(N)	3.1 Å Undefined- VDW clash	No change **Not present in A chain**
		E352(C)→ G354(N)	3.3 Å Undefined- VDW	**New bond in mutant**			**E352(C)→ G354(N)**	3.1 A Undefined- VDW clash	**New bond in mutant** **Not present in WT**
					V352(O)→ G354(N)	3.2 Å H Bond - VDW	E352(O)→ G354(N)	3.2 Å H Bond- Proximal	**Not present in A chain**
							E352(O)→ R431(N)	3.9 Å Ionic- Proximal	**New bond in mutant** **Not present in A chain**

Abbreviations and Definition: H bond: Hydrogen bond: Partial intermolecular bonding interaction between a lone pair on an electron-rich donor atom; **VDW:** Vander Waal force: Attraction and repulsions between atoms, molecules, and surfaces, as well as other intermolecular forces.

Undefined: Some kind of intramolecular forces of the element; **Proximal:** The atom of amino acids that are spatially proximal; **Ionic:** Chemical bonding that involves the electrostatic attraction between oppositely charged ions; **Elements: C**: Carbon, **O**: Oxygen, **N**: Nitrogen

Supplemental Table 6. Disruption in transcription factor binding site due to promoter mutations. The promoter sequence of the *ACS2* gene was analyzed by Plant ChIP- seq Database (PCBase; http://pcbase.itps.ncku.edu.tw**)** to predict the sites for binding of transcription factors and other DNA binding proteins. The promoter mutations altered the binding sites of transcription factors and DNA binding proteins listed below. For details, see Supplemental dataset 1.

Mutated base position on *ACS2* promoter	**Binding site in WT**	**Binding sites in *acs2- 2* mutant**	**Remarks**
-106 ± 4	1. SOC1 2. ABF4	1. AZF 2. ABF4	Lost SOC1 binding and gained AZF transcription factor binding AZF has strong homology with tomato Zinc finger, C2H2- type transcription factor (Solyc04g077980.1), a putative transcriptional repressor
-382 ± 4	1. 3-SEP 2. ZmCCA1B	1. 3-SEP 2. ZmCCA1B	No change

Immink RG, Posé D, Ferrario S, Ott F, Kaufmann K, Valentim FL, De Folter S, Van der Wal F, van Dijk AD, Schmid M, Angenent GC. (2012) Characterization of SOC1's central role in flowering by the identification of its upstream and downstream regulators. *Plant Physiology* **160**: 433- 449.

Kodaira KS, Qin F, Tran LS, Maruyama K, Kidokoro S, Fujita Y, Shinozaki K, Yamaguchi-Shinozaki K. (2011) Arabidopsis Cys2/His2 zinc- finger proteins AZF1 and AZF2 negatively regulate abscisic acid- repressive and auxin-inducible genes under abiotic stress conditions. *Plant Physiology* **157**: 742- 756.

Supplemental Table 7. Changes in methylation status of *ACS2* promoter at -106 and -382 position during fruit ripening. The methylation data were downloaded from Tomato Epigenome Database (http://ted.bti.cornell.edu/epigenome/index.html). The table lists the methylation status at -106 and -382 position (mutated in *acs2-2*) of ACS2 promotor at different stages of fruit ripening. For the full table see Supplemental dataset 2.

Mutation Position (ITAG2.5)	Chromosome Position (ITAG2.4)		Context	MG			BR			BR+10			CNR_BR		
	Position	Strand		5mc	C	Ratio	5mc	C	Ratio	5mc	C	Ratio	5mc	C	Ratio
-106	78217288	+	CHH	2	12	14%	1	8	11%	0	2	0%	0	0	n/a
-382	78217565	-	CWG	4	1	80%	9	4	69%	1	6	14%	2	1	66%

Supplemental Table 8. Comparisons of flower numbers and fruit set in WT and *ACS2* mutants. The data was recorded for five independent plants (65-day-old) of each mutant. All flower truss present in 65-day-old plants were considered here.

Plant accession	No. of flowers/truss	Total no. of flowers/ plant	Total no. of fruit set/truss
WT (M82)	6-8	90-100	6-7
acs2-1	7-10	60-80	6-9
acs2-1/*acs2-1*	5-7	70-90	4-6
acs2-2	5-7	45-65	3-5
acs2-2/*acs2-2*	5-7	45-65	3-5

Supplemental Table 9. List of primers used for screening for mutations detection in the *ACS2* gene by TILLING. The primers used for screening for mutations by TILLING and Sanger-based sequencing were designed based on the tomato genome sequence SGN SL2.50 version. The *ACS2* gene information and location of the primers on the genome sequence is also indicated. M13 tailed primers were used for screening for the mutations in the *ACS2* gene on Li-COR 4300 DNA analyzer using TILLING.

Gene	Primer Sequence (5′→3′)		Start Position	End Position	Amplicon size
M13	Fp	TGTAAAACGACGGCCAGT			
	Rp	AGGAAACAGCTATGACCAT			
ACS2 Solyc01g095080.2.1 (Set I)	Fp	CTCGATGACCTTTAAAATCG	86457060	86457040	1080
	Rp	GAGTTGGTCTTTGCAATCTC	86456000	86455980	
ACS2 Solyc01g095080.2.1 (Set II)	Fp	TCCCTCACATTCCTTAATTCTC	86456390	86456410	1006
	Rp	TTACGCTGGGTAGTATGGTGAA	86455362	86455384	
ACS2 Solyc01g095080.2.1 (Set III)	Fp	GACCATTGCTTATCGAGGTAAAAT	86454755	86454731	924
	Rp	CGAAAGTCGATTCCCTTAAAAGT	86453808	86453831	
ACS2 Solyc01g095080.2.1 (Set IV)	Fp	TTAGCGGCAATGCTATCGGAC	86453944	86453923	850
	Rp	CACAAACACCATAATCTCTCCATCTC	86453068	86453094	
ACS2 Solyc01g095080.2.1 (Set V)	Fp	GGAGAAGGAAGGAATACGAGC	86458241	86458220	728
	Rp	TGAAGATCTTACTAGGCAC	86457514	86457533	
ACS2 Solyc01g095080.2.1 (Set VI)	Fp	CGATAGAAAAGCTCGATCAA	86457569	86457549	721
	Rp	TATTTTTACCCCTAGCCTCG	86456849	86456849	
ACS2 Solyc01g095080.2.1 (Set VII)	Fp	TGTTTGGTTGTTGGGGGTTG	86456891	86456871	687
	Rp	TACTAAATGAGTTTAGAAGTGA	86456203	86456225	

Supplemental Table 10. List of genes and the primers used for qRT-PCR analysis. The gene coordinates are according to SGN SL2.50 version. The genes are as follows: *ACS- 1-aminocyclopropane-1-carboxylate synthase (isoforms 2 and 4); ACO- 1-aminocyclopropane-1-carboxylate oxidase (isoforms 1 to 4); DXS- Deoxy-xylulose 5-phosphate synthase, PSY1- Phytoene synthase1, PDS- Phytoene desaturase, ZISO- ζ-carotene isomerase, ZDS- ζ-carotene desaturase; CRTISO- Carotenoid isomerase, LCYB1- Lycopene β-cyclase 1, CYCB- Chromoplast specific Lycopene β-cyclase, LCYE- Lycopene ε-cyclase, CRTRB2- β-carotene hydroxylase 2, ZEP- Zeaxanthin epoxidase, NCED1- 9-cis-epoxycarotenoid dioxygenase1, ETR- Ethylene receptor like protein (isoform 1 to 6); β-ACTIN, UBIQUITIN 3.*

Gene Name	Primer Sequence (5′→3′)		Start position	End position	Amplicon size (bp)
ACS2 (Solyc01g095080.2.1)	Fp	AAGCTTAACGTCTCGCCTGGAT	86453766	86453745	101
	Rp	AGCGCAATATCAACCGTTCCAT	86453289	86453267	
ACS4 (Solyc05g050010.2.1)	Fp	TATTGAAAGCGCGAAAAGGT	59890996	59891016	117
	Rp	CGCAAATCCATCCAACAATA	59891112	59891132	
ACO1 (Solyc07g049530.2.1)	Fp	AAGAGGCAGAGGAAAGTACACA	59832155	59832177	130
	Rp	GGATCACTTTCCATTGCCTTCA	59832284	59832262	
ACO2 (Solyc07g045040.2)	Fp	TAGAGCTGCTGATGGATTTGAA	58140227	58140249	92
	Rp	GCTGTCAAAAACAATCGATCAC	58140319	58140297	
ACO3 (Solyc07g049550.2.1)	Fp	GTTCTTGGAAGTTATACAAACGTAGC	59849157	59849183	80
	Rp	ACACAACAATCACACACACATACAC	59849236	59849211	
ACO4 (Solyc02g081190.2)	Fp	CTTGATTGGGAGAGCACTTTCT	45251290	45251312	81
	Rp	AGTCCAAGATTCTCACATAGC	45251670	45251649	
DXS (Solyc01g067890.2.1)	Fp	AAATGGGATCGGTGTAGAGC	76869381	76869361	115
	Rp	TGCTGAGCCATATCCCAATA	76869166	76869186	
PSY1 (Solyc03g031860.2.1)	Fp	TGAATTAGCACAGGCAGGTC	4328794	4328814	140
	Rp	TCAATTCTGTCACGCCTTTC	4328934	4328914	
PDS (Solyc03g123760.2.1)	Fp	TATCATCAACGTTCCGTGCT	70501807	70501827	122
	Rp	TATCGGTTTGTGACCAGCAT	70503519	70503499	
ZISO (Solyc12g098710.1.1)	Fp	AGAGCGTGCTTTTCGTGTATTG	66127896	66127918	107
	Rp	ATTGCCATAACTGCACTCCATC	66128113	66128091	
ZDS (Solyc01g097810.2.1)	Fp	TCCAAAAGGGCTATTTCCAC	88522265	88522245	115
	Rp	TTGATCCAAGAGCTCCACAG	88522151	88522171	
CRTISO (Solyc10g081650.1.1)	Fp	GAGATCGCCAAATCCTTAGC	62684933	62684913	118
	Rp	CAGAAAGCTTCACTCCCACA	62684184	62684204	
LCYB1 (Solyc04g040190.1.1)	Fp	CGATGCAACTGGCTTCTCTA	11947704	11947724	149
	Rp	AATGAGAATCTCGCCAATCC	11947852	11947832	
CYCB (Solyc06g074240.1.1)	Fp	TCTTCTCAAGCCTTTTCCATC	45899714	45899693	92
	Rp	TGGTGGGACTTAGAAAAGAAGG	45899623	45899645	
LCYE (Solyc12g008980.1.1)	Fp	TTAGTCGCCATTTTCTGCAC	2287554	2287584	130
	Rp	TCACCCTCGCACTCTACAAG	2287795	2287775	
CRTRB2 (Solyc03g007960.2.1)	Fp	CGCCATAACAAATGCTGTTC	2449246	2449266	148
	Rp	ATGAACCAGTCCATCGTGAA	2449477	2449457	
ZEP (Solyc02g090890.2.1)	Fp	GGTCGTGTTACATTGCTTGG	52372495	52372515	118
	Rp	TGCATGCTTTTTCAAGTTCC	52369422	52369442	
NCED1 (Solyc07g056570)	Fp	TGACACCACCAGACTCCATT	64361856	64361836	130
	Rp	ACTTGTTCATCCGGGTTTTC	64360420	64360440	

Gene Name	Primer Sequence (5′→3′)		Start position	End position	Amplicon size (bp)
ETR1 (Solyc12g011330)	Fp	GTTGCCTGCTGACGACTTGC	4168724	4168736	149
	Rp	GCACCGAACTGCACAAGAACC	4171235	4171256	
ETR2 (Solyc07g056580)	Fp	ACAAGGACTGTGGCAATGGTG	64392214	64392235	170
	Rp	GCATGAGCCGTTTTTCATCTCC	64392383	64392361	
ETR3 (Solyc09g075440)	Fp	CGCAGATCAGGTTGCTGTCG	67136394	67136374	178
	Rp	TGGGCGTTCTCATTTCATGG	67130281	67130301	
ETR4 (Solyc06g053710)	Fp	AGCCAGAGGGGACCATGTTG	6555571	6555551	169
	Rp	CCTTGGAGGAGTGAGTGTGG	6553123	65531413	
ETR5 (Solyc11g006180)	Fp	ATTCGGATGCCACTGCTTCG	928889	928869	173
	Rp	GGATAAAGCCACAGCCACCTG	927887	927908	
ETR6 (Solyc09g089610)	Fp	CCCCTGCTCCTCCAACATACG	69359479	69359492	149
	Rp	GCATGGCTGTGATTGTCGGAT	69361385	69361364	
β-ACTIN (FJ532351.1)	Fp	GTCCCTATTTACGAGGGTTATGC			108
	Rp	CAGTTAAATCACGACCAGCAAGATT			
UBIQUITIN 3 (X58253.1)	Fp	GCCGACTACAACATCCAGAAGG			110
	Rp	TGCAACACAGCGAGCTTAACC			